Accepted Manuscript

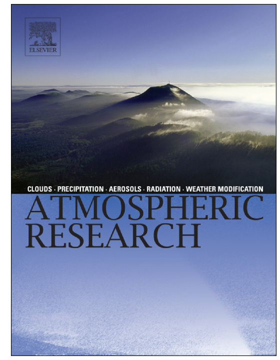

Assessment of atmospheric aerosols from two reanalysis products over Australia

S.K. Mukkavilli, A.A. Prasad, R.A. Taylor, J. Huang, R.M. Mitchell, A. Troccoli, M.J. Kay

PII: S0169-8095(18)30123-6
DOI: doi:10.1016/j.atmosres.2018.08.026
Reference: ATMOS 4356

To appear in: *Atmospheric Research*

Received date: 11 February 2018
Revised date: 4 July 2018
Accepted date: 31 August 2018

Please cite this article as: S.K. Mukkavilli, A.A. Prasad, R.A. Taylor, J. Huang, R.M. Mitchell, A. Troccoli, M.J. Kay , Assessment of atmospheric aerosols from two reanalysis products over Australia. Atmos (2018), doi:10.1016/j.atmosres.2018.08.026

This is a PDF file of an unedited manuscript that has been accepted for publication. As a service to our customers we are providing this early version of the manuscript. The manuscript will undergo copyediting, typesetting, and review of the resulting proof before it is published in its final form. Please note that during the production process errors may be discovered which could affect the content, and all legal disclaimers that apply to the journal pertain.

ACCEPTED MANUSCRIPT

Assessment of atmospheric aerosols from two reanalysis products over Australia

S. K. Mukkavilli[1,2], A. A. Prasad[3], R. A. Taylor[1,4], J. Huang[2], R. M. Mitchell[2†], A. Troccoli[5,6], and M. J. Kay[1]

[1]School of Photovoltaic and Renewable Energy Engineering, University of South Wales (UNSW), Australia.

[2]Oceans and Atmosphere, Commonwealth Scientific and Industrial Research Organisation (CSIRO), Canberra, Australia.

[3]Climate Change Research Centre and Australian Research Council (ARC) Centre of Excellence for Climate System Science, University of New South Wales (UNSW), Australia.

[4]School of Mechanical and Manufacturing Engineering, University of South Wales (UNSW).

[5]School of Environmental Sciences, University of East Anglia (UEA), Norwich, UK.

[6]World Energy & Meteorology Council, c/ UEA, Norwich, UK.

Corresponding author[1]: Surya Karthik Mukkavilli (karthik.mukkavilli@student.unsw.edu.au)

Abstract

Assessments of atmospheric aerosols from reanalysis are important for understanding uncertainty in model simulations, and ultimately predictions, such as for solar power or air quality forecasts and assessments. This study intercompares total aerosol optical depth (AOD) and dust AOD (DAOD) from two global reanalyses datasets, the European Centre for Medium-Range Weather Forecasts (ECMWF) Monitoring Atmospheric Composition and Climate (MACC) and the NASA Modern-Era Retrospective Analysis for Research-2 (MERRA-2). These are evaluated against AeroSpan (Aerosol characterisation via Sun photometry: Australian Network) ground observations which forms part of the Aerosol Robotic Network (AERONET) over the Australian continent for the 2002-2012 period. During dust storms, AeroSpan/AERONET AOD measurements were missing due to cloud screening. To overcome validation limitations in sun photometry for dust events, a nephelometer's scattering coefficient is qualitatively compared against reanalysis of DAOD at a key dust storm activation site, Tinga Tingana in South Australia (~200km east of Lake Eyre). A specific extreme event that occurred in 2009 originating from the Lake Eyre basin, a major dust source covering one-sixth of Australia, was studied. The results show that

†Deceased 13 April 2018
[1]Permanent address: karthik@groundobs.com

ACCEPTED MANUSCRIPT

MERRA-2 reanalysis overestimates monthly total AOD twice as much compared to AeroSpan/AERONET ground observations but seems better correlated against AeroSpan/AERONET than ECMWF/MACC. Mean data of MERRA-2 time series over 10 years provide lower DAOD values and lower dust aerosol estimates than ECMWF/MACC reanalysis (over the Lake Eyre basin with spatial averaging). Specifically at Tinga Tingana, the correlation from MERRA-2 (0.45 correlation) and ECMWF/MACC (0.43 correlation) against AeroSpan/AERONET's AOD were similar. Between MERRA-2 and ECMWF/MACC decade long daily gridded DAOD, the correlation coefficient was high at 0.73, again indicating similarity between the datasets. MERRA-2 total AOD correlation is significantly higher (by 0.26) against AeroSpan/AERONET than ECMWF/MACC. MERRA-2 also provides higher AOD values in extreme cases which may correspond to dust storms. During dust storms, a hybrid strategy using nephelometers and hourly reanalysis from MERRA-2 is able to identify dust storms better than AeroSpan/AERONET. Overall, this work can enable and inform better aerosol data assimilation into forecast models such as for solar energy, agriculture or air quality over Australia.

Keywords

reanalysis; aerosol optical depth; AERONET; Australian dust AOD; ECMWF/MACC; MERRA-2

1. Introduction

Aerosols have been recognised as a large source of uncertainty in climate change projections (Boucher et al., 2013; Choobari et al., 2014) and they must be known to accurately estimate the amount of solar resource available for solar energy applications (e.g. Perry and Troccoli, 2015; Toll et al., 2016; Alexandri et al., 2017, Mukkavilli et al., 2017; Beegum et al., 2018). Advances in satellite retrievals, models and assimilations have resulted in demonstrably better reanalysis products (Levy et al., 2010; Gillingham et al., 2012; Molod et al., 2015; Qin et al., 2015; Gelaro et al., 2017; Ridley et al., 2016).

Australia is the largest source of airborne dust aerosol in the Southern Hemisphere (Tanaka and Chiba, 2006). According to Tanaka and Chiba (2006), Australia's dust contributes 5.7% of 1877 Tg yr^{-1} global dust emissions. Dust accounts for ∼30 % of the total global aerosol mean direct radiative effect (DRE) (Heald et al., 2014). At the same time, there is significant uncertainty in the value and direction of radiative forcing of dust, estimated to be anywhere between −0.3 and +0.1 Wm^{-2} (Boucher et al., 2013). Furthermore, observations show that the occurrence and intensity of dust from Australia has substantial variability at seasonal, interannual, and decadal timescales (Goudie and Middleton, 1992; Leys et al., 2008; Strong et al., 2010). Therefore, dust and total aerosol emissions, which includes dust, biomass and other aerosols, from Australia are critical for quantifying the overall uncertainty associated with the Southern Hemisphere aerosol and the global albedo.

The significance of Australian dust is also well-recognised for local climate impacts (Evans et al., 2016). Dust from Lake Eyre and its surrounding basin (centered at 28.4°S, 137.4°E) has been shown to impact precipitation (Rotstayn et al., 2011) and air quality (Chan et al., 2005; Leys et al., 2011) in Australia, while farther downwind it is important to the productivity of the Tasman Sea and Southern Ocean (Boyd et al., 2004; Gabric et al., 2010). Its accumulation is used as a paleoclimate proxy in New Zealand (Marx et al., 2009) and Antarctica (Revel-Rolland et al., 2006). Dust is a strong driver of regional climate near and downwind from source regions (Shao et al., 2011). Scattering and absorption of radiation by dust in the atmospheric column impacts surface energy fluxes and the stability of the atmosphere, while deposition of dust from the atmosphere to the ocean is important to biogeochemical cycles. Rotstayn et al. (2012) investigated feedbacks related to dust by comparing two 160-year coupled atmosphere-ocean simulations of modern-day climate using the CSIRO Mark 3.6 global climate model (GCM). They found that inclusion of interactive dust in their model amplifies the impact of the El Niño–Southern Oscillation (ENSO) cycle on the Australian climate, with longer and hotter droughts and more intense wet periods.

Australian dust sources have been well studied from a topographic perspective (Leys et al., 2008; Bullard et al., 2008), from geological surveys analysing landscape changes and wind erosion (McTainsh et al., 1998; O'Loingsigh et al., 2015b) to characterising aerosol via sun photometry (Mitchell et al., 2017). The CSIRO operates a ground station network, the Aerosol characterisation via Sun photometry: Australian network (AeroSpan), which forms part of the Australian component of AERONET, a worldwide sun photometer network operated by NASA (Holben et al., 1998). In analysing sun photometer data, Mitchell et al. (2017) identified continental aerosol classified in the arid zone has a larger periodic component, with pronounced twin spring-summer peaks, and an increasing episodic component towards active dust source regions. Mitchell et al. (2010) analysed sun photometer and nephelometer measurements from Tinga Tingana (28.80°S, 140.167°E), near the Lake Eyre Basin in the Australian desert and the arid centre of the continent during the Millennium drought (2002-2010). They found an approximate doubling in both column AOD and near-surface aerosol nephelometer readings during the summer months (DJF) over the duration of the drought. Whenever there is a major dust storm from the Lake Eyre Basin (the source of most dust aerosols in the Southern Hemisphere), Tinga Tingana was found to be an active dust site (O'Loingsigh et al., 2015a).

With this recent progress in characterising Australian continental columnar AOD via sun photometry, it is now possible to conduct long-term validations of model outputs and reanalysis AOD over regions of the Australian continent. However, AeroSpan/AERONET sites are still quite sparse over the Australian continent although maritime aerosol has been studied extensively over the ocean (Gras and Ayres, 1983; Gras, 1991). Therefore, barely sufficient AOD data is now available to conduct climate and remote sensing climatological validation studies over the continent.

1.1 Reanalysis models

Reanalysis products are obtained using a fixed data assimilation scheme and a global climate model which ingest all available observations every 6-12 hours. Reanalysis of aerosol

ACCEPTED MANUSCRIPT

over Australia is promising as it assimilates satellite retrievals to provide extensive areal and temporal gridded coverage available over a sparsely-populated continent. Relying only on satellite data can present problems. For example, the dense-dark vegetation (DDV) assumption inherent in the Moderate Resolution Imaging Spectroradiometer (MODIS) aerosol retrieval 15 algorithm does not apply well over most of Australia (Levy et al., 2010; Gillingham et al., 2012). Problems in other sensors and retrieval methods of satellites are discussed by Qin et al. (2015). Reanalysis products can potentially address these issues through assimilating multiple sources. Alternatively, reanalysis can be inaccurate due to various issues including limitations in model physics, resolution and the underlying sources used for assimilation. Therefore, rather than using reanalysis AOD values as the direct truth, reanalysis approaches must also be verified and intercompared.

A comprehensive intercomparison study of reanalysis datasets against AeroSpan/AERONET over Australia is currently lacking. There has been one recent global study by Ridley et al. (2016) – a five-year observational assessment of seasonal dust AOD with hybrid satellite, a single reanalysis and model output predictions of dust over Australia was performed. They estimated that the global dust AOD at 550 nm is 0.030±0.005, higher than the AeroCom model median (0.023) and substantially narrowing the uncertainty (Huneeus et al., 2011). However, differences between these model simulations are substantial, with estimates of global dust aerosol optical depth (AOD) that vary by a factor of over 5. Ridley et al. (2016)'s hybrid dust AOD study is useful to compare against reanalysis datasets since sun photometer sites over Australia are sparse, and these only provide total AOD, filtering out AOD during dust storms and no dust AOD component. Nonetheless, they had particularly large error bars indicating high uncertainty of aerosols over the Australian continent, despite being only a seasonal assessment. Their seasonal dust AOD in South America, South Africa and Australia were close to the model noise, indicating low dust AOD and high uncertainty (because the low dust AOD estimate could just be disguised by noise). However, given Australia's dust contributes substantially to global dust emissions (5.7%, see

ACCEPTED MANUSCRIPT

Tanaka and Chiba, 2006), the uncertainty over Australia from Ridley et al. (2016) is unsatisfactory. One possible reason for this uncertainty is the lower landmass in the Southern Hemisphere and sparser ground measurements for bias corrections over Australia. Therefore, this study further investigates dust AOD with other reanalysis datasets at higher spatiotemporal resolutions than seasonal comparisons in Ridley et al. (2016) against AeroSpan/AERONET sites and with longer decadal time series. Secondly, Ridley et al. (2016) did not consider daily or sub-daily dust aerosol which is typically the time period over which dust storms occur. Exploring dust and total AOD reanalysis at higher resolutions is necessary to providing a more accurate assessment of biases against ground observations.

To bridge these gaps, our study explores reanalysis datasets at higher spatial and temporal resolutions by focusing on daily time frames. Secondly, we also intercompare reanalysis datasets in Australia grid-wise rather than with a regional average (as was done in Ridley et al. (2016)) in addition to intercomparing at up to hourly timescales. At present, there is a large uncertainty around how different gridded AOD datasets compare against each other and against ground observations over the Australian continent. Therefore, the key objectives of this paper are as follows:

- Assessment of decadal aerosol reanalysis datasets over Australia against key dust activation AeroSpan/AERONET site Tinga Tingana in Lake Eyre basin (up to daily time scales)
- Intercomparisons of time series and spatial differences between ECMWF Monitoring Atmospheric Composition and Climate (MACC) (Inness et al., 2013a) and Modern-Era Retrospective analysis for Research and Applications-2 (MERRA-2) (Buchard et al., 2017; Gelaro et al., 2017; Randles et al., 2017) AOD reanalysis
- Seasonal comparison of MERRA-2 dust aerosol optical depth (DAOD) reanalysis against global dust source model hybrid (dust source + non-dust model) outputs (Ridley et al., 2016)

ACCEPTED MANUSCRIPT

2. Data

This study utilises datasets from various sources, including hybrid models, reanalysis and ground observations, to analyse dust AOD, total AOD, and extinction coefficient. An overview of datasets used in this study is provided in Table 1. The datasets analysed were over a decade, and correspond to AeroSpan/AERONET sites around Australia. The AeroSpan/AERONET sites of interest are shown in Figure 1, which also shows the modified domain used which is similar to that of Ridley et al. (2016) (35S, 120E to 20S, 150W) to provide the highest coverage of ground sites relevant to dust source regions over Australia. The datasets have been analysed from hourly to seasonal frequencies. As shown in Table 1, the dataset used from Ridley et al. (2016) is a hybrid model over a five-year period with seasonal mean frequency averaged over the domain in Figure 1. MERRA-2 and ECMWF are both gridded reanalysis products with spatiotemporal datasets extracted over the entire domain in Figure 1. We extract data from a single grid point closest to the AERONET site of investigation at the best range of dataset frequencies available. Thus, the reanalysis datasets range from 3-hourly to monthly as required for intercomparisons stated in the objectives of this study – decadal reanalysis versus AeroSpan/AERONET at Tinga Tingana; intercomparison of time series and spatial differences between reanalysis; and seasonal comparison against Ridley et al. (2016). Finally, the AeroSpan/AERONET measurements used monthly (climatology) data for all four sites in Fig. 1 and additionally at key dust activation site Tinga Tingana (see Fig. 1, reproduced from O'Loingsigh et al., 2015a), a higher temporal resolution of daily average AOD was also analysed for over a decade.

We performed pointwise comparisons against available measurements at the four sites shown in Fig. 1, where AERONET is assumed to provide the true total AOD. The reanalysis grid point closest to the ground site was assessed for the duration of the AERONET datasets. For this assessment, since MERRA-2 AOD outputs are at 550 nm whereas AERONET is 500 nm AOD, the monthly averaged angstrom (α) available from AERONET between 440-870

ACCEPTED MANUSCRIPT

nm can be used to approximate the AERONET value at 550 nm AOD as shown in equation 2:

$$AOD_{550nm} = AOD_{500nm} * (550/500)^{-\alpha} \quad (2)$$

Thus, the AOD 550 nm approximation was tested in addition to the 500 nm AOD to validate MERRA-2 at 550 nm at all sites as a monthly time series. The differences in AOD correlation at the AERONET 500 nm wavelength will be compared against the modified angstrom based AOD 550 nm approximation to evaluate the more suitable wavelength for Tinga Tingana based on correlations and biases against reanalysis.

Moreover, a unique feature of this AERONET analysis is the ability to extract a continuously operating nephelometer dataset during a major dust storm event over Tinga Tingana. This additional source of data has the potential to alleviate limitations in sun photometry for dust storm detections due to the gaps in ground observations. This nephelometer feature of AeroSpan/AERONET will be further investigated in this study along with its ability to work in conjunction with other reanalysis sources of data to better validate dust storms. Sections 2.1-2.3 will provide further information about the sources presented in Table 1.

Table 1. Dataset sources; type and resolution; aerosol variables; frequency of measurements; time period of measurements; and domain or AeroSpan/AERONET sites considered

Source	**Type**	**Variable**	**Frequency**	**Period**	**Domain/Site**
Ridley et al. (2016) MIT-UCLA-PNNL study	16 Hybrid dust source + non-dust spatial average Monte Carlo model outputs	DAOD 550 nm	Seasonal mean	2003 Dec-2008 Nov	(35S, 120E to 20S, 150W)
MERRA-2 (GMAO, 2015a, 2015b, 2015c)	Gridded Reanalysis $0.5^{o}x0.625^{o}$	DAOD 550 nm	Monthly mean	2003-2008	(35S, 120E to 25S, 150W)
		Total AOD 550 nm	3 hourly instant	2003-2008	(35S, 120E to 25S, 150W)
	Reanalysis grid point $0.5^{o}x0.625^{o}$ closest to AeroSpan/AERONET site	Total AOD 550 nm	Monthly mean	2002-2012	Tinga Tingana
				2005-2016	Birdsville
				2013-2016	Flowers Gap
				2012-2016	Lake Lefroy

ACCEPTED MANUSCRIPT

		Total AOD 550 nm	24h mean	2002-01-01 to 2016-11-30	Tinga Tingana
			3 hourly instant	2002-01-01 to 2016-11-30	Tinga Tingana
ECMWF/ MACC (Inness et al., 2013b)	Gridded Reanalysis 0.125°	DAOD 550 nm	3 hourly instant	2003-2008	(35S, 120E to 25S, 150W)
	Reanalysis grid point 0.125°	DAOD 550 nm	3 hourly instant	2003-2012	Tinga Tingana
		Total AOD 550 nm	3 hourly instant	2003-2012	Tinga Tingana
AeroSpan/ AERONET v2 (2018) (Holben et al., 1998)	Aerosol Observations	Total AOD 500 nm	Monthly mean	2002-2012	Tinga Tingana
				2005-2016	Birdsville
				2013-2016	Flowers Gap
				2012-2016	Lake Lefroy
		Total AOD 500 nm	24h mean	2002-2012	Tinga Tingana
	Nephelometer (2009 Australian dust storm event)	Scattering Coefficient (Mm^{-1})	Continuous	Sep 21- Sep 22 2009	Tinga Tingana

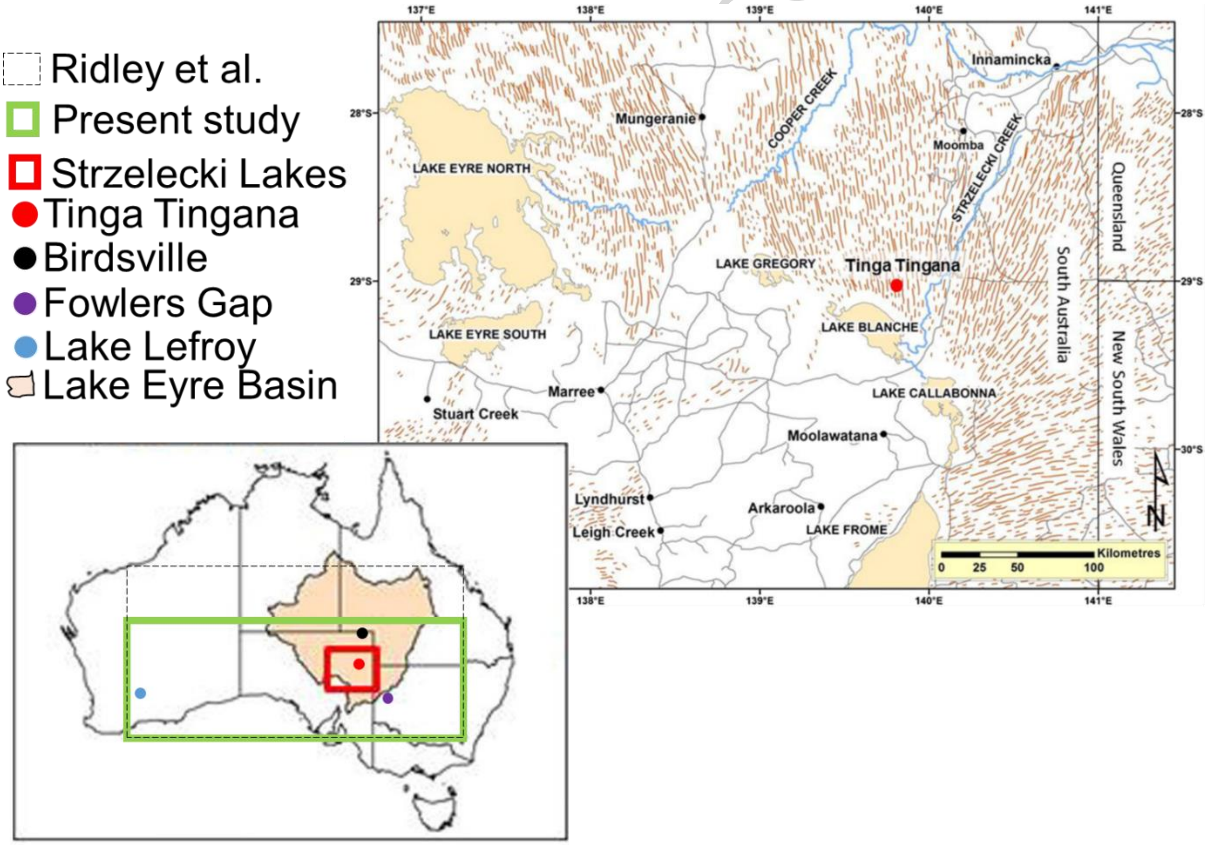

Figure 1. Gridded AOD: reanalysis domain from Ridley et al. (2016) global observationally constrained dust AOD estimate study over Australia (black dotted box: 35S, 120E to 20S, 150W); reduced domain size in this study (green box: 35S, 120E to 25S, 150W) which still covers all AeroSpan/AERONET ground sites; Strzelecki Lakes region (red box) within the Lake Eyre Basin (shaded) relative to the Australian continent zoomed in to show AERONET/AeroSpan station at Tinga Tingana (red dot); AERONET/AeroSpan at Tinga Tingana (red dot), Birdsville (black dot), Fowlers Gap (violet dot) and Lake Lefroy (blue dot) stations (reproduced from Fig. 1 in O'Loingsigh et al., 2015a)

2.1 Ground AOD Measurements

ACCEPTED MANUSCRIPT

Aerosol ground measurement stations on the Australian continent are sparse. Aerosol total optical depth measurements were obtained at four locations across the Australian continent between 2002 and 2016, as indicated in Figure 1. It should be noted that AeroSpan/AERONET cannot provide component-specific optical depth information (e.g. dust AOD). The AeroSpan/AERONET (Table 1) column shows the beginning and end date and the periodicity of measurements at each site considered. The data used is the total AOD daily average level 2, version 2, direct sun algorithm which is cloud screened (Holben et al., 2006). The AeroSpan/AERONET sun photometers are manufactured by Cimel CE-318 and the standardised spectral channel instrument output closest to visible at 500 nm was used. Further information regarding the quality assurance criteria for AERONET's Version 2.0 is provided by Holben et al. (2006).

Several major improvements have led to the release of Version 2.0. This includes significant changes to the inversion code, the input data and the criteria for quality assurance that notably depart from Version 1.0. Most significant among the inversion code changes is that the spherical and spheroid model outputs are internally evaluated to produce one set of retrievals rather than two products as in Version 1.0. In that regard Version 2.0 provides a parameterisation of the degree of non-sphericity (Dubovik et al., 2006). Noteworthy among the input changes is the characterisation of surface albedo.

2.1.1 2009 Australian Dust Storm Observations

Dust storms are often associated with large scale synoptic events like frontal systems and storms which create strong winds to blow the dust, which then produce large clouds of dust. These dust clouds make sun photometry inherently unsuitable for detecting dust storms. Moreover, AERONET applies a cloud screening algorithm. However, in Australia the AERONET network also contains a continually operating nephelometer at Tinga Tingana, installed in 1998 to complement the AERONET Cimel sun photometer enabling continuous measurement of near surface scattering. The nephelometer samples the concentration of

ACCEPTED MANUSCRIPT

suspended particulate matter in ambient air 2 meters above the surface. The instrument response is reported as the scattering coefficient σ_{sca} in units of inverse megametres (Mm^{-1}). Application of nephelometer data to dust haze measurements and its relation to other pollution indices such as particulate mass loading is widely applied in air quality monitoring (Kim et al., 2001; Zhu et al., 2015; Szczepanik and Markowicz, 2018).

Nephelometer measurements are not impeded by cloud cover and the nocturnal void implicit in sun-photometry used to measure aerosol optical depth (or extinction). The Tinga Tingana instrument is located 40 km north-east to the closest of the Strzelecki lakes, Lake Blanche (Fig. 1). This lack of exact collocation raises the question of the capacity of a single point measurement to represent broad-scale dust mobilisation across the Strzelecki Lakes. Furthermore, the measurement is made at a single height of 2 meters, whereas the satellite images receive scatter radiance from all heights. These issues are addressed by O'Loingsigh et al. (2015a) who noted that any day of visible dust activity in the Lake Eyre Basin, regardless of the number or types of sources involved, is nearly always included the Strzelecki Lakes. Hence, although dust plumes from the lakes may not always pass directly over the nephelometer, the recording of dust by this instrument from any direction is a good indicator of dust mobilization occurring at the lakes. Mitchell et al. (2010) previously compared the nephelometer record with observer-based estimates of dust storms occurring anywhere in the Lake Eyre basin (LEB) on a given day, quantified by Bullard et al. (2008) as 'dust storm days' or DSDs. This comparison showed that ~50% of the DSDs listed by Bullard et al. (2008) were associated with 'significant' events at Tinga Tingana, suggesting a high level of basin-wide dust mobilization. Since the LEB is ~800 km in both zonal and meridional directions, this result is particularly relevant to the present study, which considers dust mobilisation over a much more local scale – the sub-basin comprising the Strzelecki Lakes – only tens of kilometres distant from Tinga Tingana. Thus, also in this study the scattering coefficient (Mm^{-1}) data was analysed at Tinga Tingana for an extreme dust event. In particular, we investigate the 2009 Australian Dust Storm during the peak of the event

ACCEPTED MANUSCRIPT

between Hour 8 of 20 Sep to Hour 12 of 22 Sep (UTC). Operation of the nephelometer in its outback setting was described in detail by Mitchell et al. (2009).

The scattering coefficient definitions also used in this study are provided in O'Loingsigh et al. (2015a) who identified dust events from MODIS "Quick-Look" imagery and compared it with the level of dust mobilisation. To determine the minimum scattering coefficient values associated with the Quick-Look analyses they recorded nephelometer response associated with the three intensity classes. O'Loingsigh et al.'s (2015a) analysis suggested a threshold of 50 Mm^{-1} as indicative of dust deflation just detectable from Quick-Look imagery. Hence this value forms the lower bound for 'Minor' events. The correlation of higher intensity dust events between Quick-Look images and the nephelometer response was more straightforward as the degree of local to regional to basin-wide dust mobilization increases with event intensity. Analysis showed that 'Moderate' events identified from the Quick-Look images were associated with $300 < \sigma_{sca} < 3000$ Mm^{-1}, with 'Major' events exhibiting $\sigma_{sca} > 3000$ Mm^{-1}.

2.2 Description of aerosol gridded reanalysis Australian dataset

2.2.1 ECMWF/MACC reanalysis

As part of the "Global and regional Earth-system Monitoring using Satellite and in situ data" (GEMS) project (Hollingsworth et al., 2008), the ECMWF developed its assimilation system to include observations pertaining to greenhouse gases, reactive gases and aerosols. Forecast values are archived for 3, 6, 9, and 12 h lead time. Model resolution is 1.125° × 1.125° grid.

In the present study Aerosol reanalysis was obtained for total and dust AOD component at 550 nm from ECMWF/MACC dataset (Inness et al., 2013b) for the entire duration available starting from January 2003 to December 2012. The ECMWF Integrated Forecast System (IFS) field outputs at highest spatial (0.125° or 14 km) grids, and temporal resolution (instantaneous 3 hourly) outputs available were extracted over the domain, (35S, 120E to

25S,150W), shown in Figure 1. This domain is similar but reduced from Ridley et al. (2016) global study over Australia to increase ground site coverage to spatial area.

The simulation assimilates total aerosol optical depth data at 550 nm from MODIS on board of Terra and Aqua satellites (data collection 5). For a general description of MODIS AOD, see Remer et al. (2005), and for a description of the current MODIS AOD collection 5 data over land, see Levy et al. (2007). The original MODIS retrievals have a resolution of 10 × 10 km^2. Since the ECMWF IFS analysis are at approximately 120 × 120 km^2, MODIS AOD data of a grid of 0.5° × 0.5° are taken. MODIS data are taken at the original time, and at the specific observation location, and model aerosol fields are interpolated to this location.

2.2.2 MERRA-2 reanalysis

The Modern-Era Retrospective analysis for Research and Applications-2 (MERRA-2) was undertaken by NASA's Global Modeling and Assimilation Office (GMAO) with two primary objectives: to place observations from NASA's Earth Observing System (EOS) satellites into a climate context and to update the MERRA system to include the most recent satellite data. Details of the evaluation of MERRA-2 aerosols, major findings and recommendations to users of the MERRA-2 aerosol products are outlined along with a summary and assessment of data assimilation by Gelaro et al. (2017), Randles (2017), and Buchard et al. (2017).

In this study, the second reanalysis dataset used is the NASA MERRA-2 (Gelaro et al. (2017) at 0.5^{o} latitude x 0.625^{o} longitude (55.8 km x 69.8 km) with the same temporal resolution and domain settings as ECMWF/MACC dataset for 550 nm total AOD. The dust AOD was obtained every month from Dec 2003 to Nov 2008 to verify against Ridley et al. (2016) dust AOD estimates.

2.3 Hybrid (satellite or reanalysis source + model) Dust AOD observation estimates – Ridley et al. model

ACCEPTED MANUSCRIPT

Ridley et al. (2016) used multiple satellite platforms, in situ AOD observations and four state-of-the-science global models to produce sixteen hybrid combinations of different satellite or reanalysis dust data sources plus model outputs to estimate dust AOD globally. The global aerosol models provide a range of estimates for the non-dust aerosol AOD and the spatial distribution of dust aerosol. Their methodology used provides regional, seasonal dust AOD and the associated statistical uncertainty for key dust regions around the globe against which model dust schemes can be evaluated in the present study. Ridley (2016) et al.'s study is a Monte Carlo observationally constrained three monthly estimate of average DAOD between Dec 2003 to Nov 2008 over the four seasons (DJF, MAM, JJA, SON). The DAOD estimate is annually and spatially averaged over the entire domain (adopted for this study) shown in Figure 1. Since ground observations do not contain dust AOD estimates, and they are cloud screened and sparse over Australia, dust AOD information from the Ridley (2016) study for all 16 model configurations was extracted seasonally over Australia from their global study over the five-year period, 2003 Dec–2008 Nov for comparison against our reanalysis and ground observations in Sections 2.1-2.2 (see Figure 2a).

For spatial averaging, they simply calculate the mean over the region for each iteration of the Monte Carlo dust AOD calculation. The 200 regional averages that are created by sampling the uncertainty distributions of the parameters are then averaged to give the estimate dust AOD for the region with the uncertainty – which in the case of Australia is often larger than the mean. The uncertainty distribution for each of these three variables, bias correction, satellite $\log_{10}$(AOD), and model non-dust $\log_{10}$(AOD), is sampled and the average dust AOD is calculated for each region.

Using the same data as in Fig. 2a, Fig. 2b provides an overview of DOAD source plus model by indicating overall DOAD uncertainty through cumulative highest to lowest DAOD estimates annually. Highest DAOD estimates were with CESM+CESM followed by GEOSChem+GEOSChem and lowest was Terra+MERRAero.

ACCEPTED MANUSCRIPT

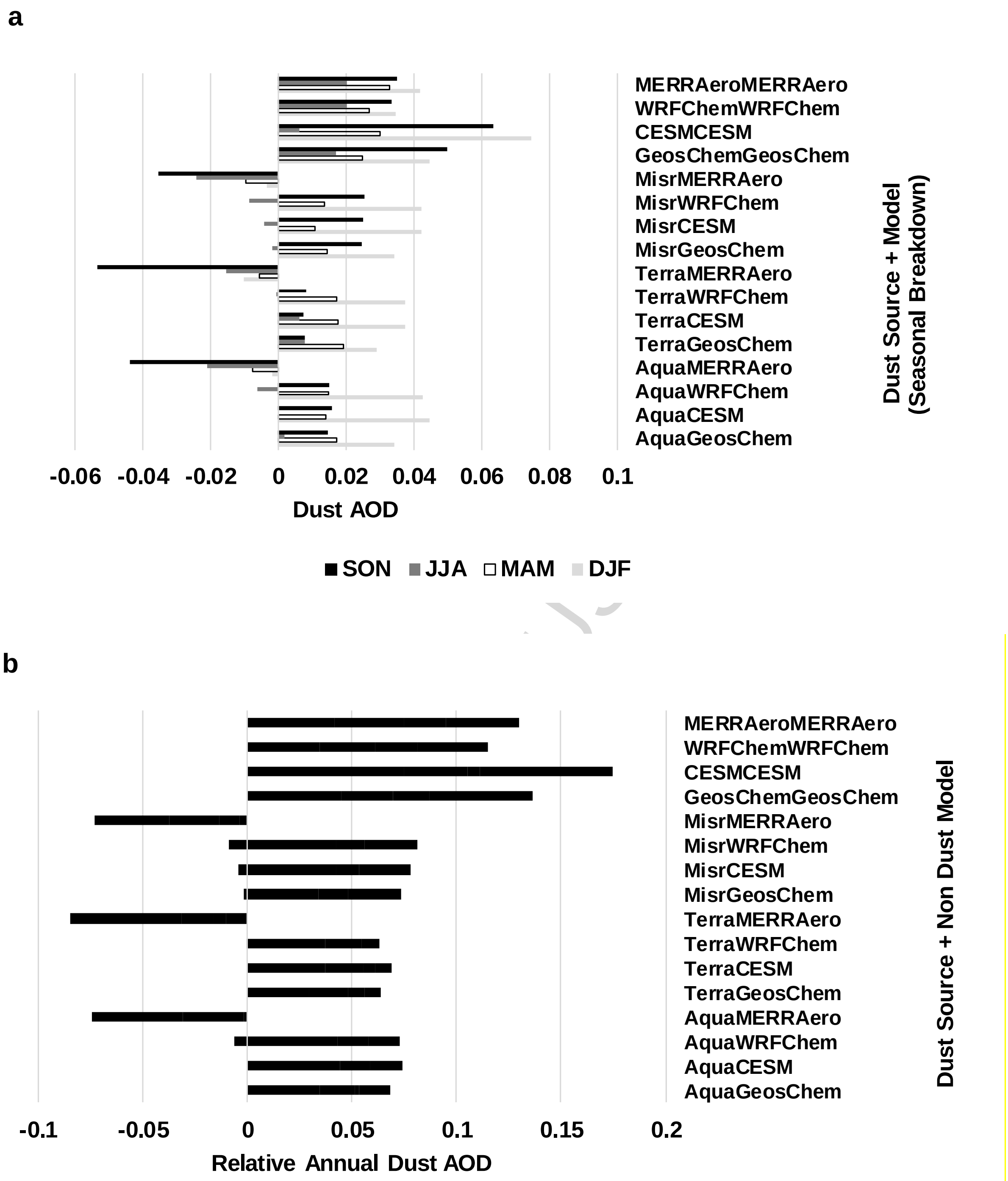

Figure 2. a. Different satellite/reanalysis dust data sources + model estimates of DAOD seasonal estimate of 2004-2008 spatial average over Australia (35S, 120E to 20S, 150W) (simplified from original annual breakdown for brevity) of a. DAOD vs season (summer (DJF); autumn (MAM); winter (JJA) & spring (SON)) b. Annual dust AOD comparison across the hybrid dust AOD estimators, y-axis: hybrid (sources + model) name; x-axis average annual (black) dust AOD estimate. Overall, the bar chart shows uncertainty range of Australian dust AOD from hybrid estimate (Ridley et al., 2016)

Table 2 provide the values of the area averaged estimate datasets from Figure 2. Ridley et al. (2016) on request provided more detailed simulation data over Australia than presented in their manuscript appendix over Australia on a yearly basis, and we averaged the data provided to us over the five-year period to produce values displayed in Table 2. For Table 2, in summer (DJF) the range of mean seasonal DAOD is -0.01 to 0.075. The variation across the years was from -0.0136 (in 2007) to 0.088 (in 2008) (CESM+CESM). Lowest estimates were with Terra+MERRAero and highest with CESM+CESM in both cases. Over Winter (JJA) the mean range in Table 2 was from -0.0244 to 0.0202. However, the actual range is from -0.0229 (in 2006) to 0.021 (in 2008). The lowest range in Table 2 was with MISR+MERRAero and MISR+MERRAero was the highest. From Figure 2 we can see that the hybrid observational estimate study allows negative estimates to prevent a positive bias in the data as shown in Eq. 1. Negative hybrid estimates are generally the result of using MERRAero as the non-dust AOD model. Non-dust refers to all other aerosol components than dust which contribute to the total AOD. The negative dust AOD estimate occurs from the hybrid if the model has higher non-dust AOD predictions than the total AOD from the source (satellite or reanalysis).

$$\text{If } \{\text{Non-DAOD}_{\text{model}} > \text{Total AOD}_{\text{source}}\} \xRightarrow{\textit{Hybrid estimate}} -|\text{DAOD}| \quad (1)$$

Obviously, these negative estimates are not ideal, but it is why multiple hybrid estimates are used to provide a more realistic dust AOD estimate. It is also why their method is expected to be generally more suited to regions with substantial mean dust loading.

Table 2. Five-yearly average data [obtained as annual results on request from Ridley et al. (2016) from graphs presented in their manuscript's supporting Appendix of Monte Carlo simulations] providing the dust AOD hybrid estimate values of Australia (35S, 120E, to 20S, 150E) over seasons, summer (DFJ), Spring (MAM), Winter (JJA) and Autumn (SON)

Sources + Model	**DJF**	**MAM**	**JJA**	**SON**
Aqua+GeosChem	0.0344	0.0173	0.0020	0.0148
Aqua+CESM	0.0446	0.0139	0.0000	0.0159
Aqua+WRFChem	0.0428	0.0149	-0.0061	0.0151
Aqua+MERRAero	-0.0020	-0.0076	-0.0212	-0.0438
Terra+GeosChem	0.0292	0.0192	0.0078	0.0077
Terra+CESM	0.0375	0.0176	0.0061	0.0075
Terra+WRFChem	0.0375	0.0172	-0.0007	0.0082
Terra+MERRAero	-0.0102	-0.0057	-0.0155	-0.0533

Misr+GeosChem	0.0342	0.0144	-0.0018	0.0247
Misr+CESM	0.0423	0.0108	-0.0040	0.0249
Misr+WRFChem	0.0422	0.0137	-0.0087	0.0255
Misr+MERRAero	-0.0035	-0.0098	-0.0244	-0.0356
GeosChem+GeosChem	0.0448	0.0248	0.0172	0.0498
CESM+CESM	0.0748	0.0302	0.0064	0.0636
WRFChem+WRFChem	0.0345	0.0270	0.0201	0.0335
MERRAero+MERRAero	0.0419	0.0330	0.0202	0.0351

3. Results

3.1 Intercomparing reanalysis against ground observations

We performed a monthly analysis of total MERRA-2 reanalysis AOD across all sites in Fig. 1 against ground observations. Figure 3a-d show the associated bias between the reanalysis and ground measurement at the corresponding time at the relevant site. As can be seen the availability of data at each site is highly variable.

The longest datasets were available at Birdsville and Tinga Tingana. These two sites also showed the highest range of total AOD biases out of the time series considered. However, this may be because of the longer duration of datasets allowing scope for more extreme values. Based on the generally positive biases, with the exception of a few months at Tinga Tingana, MERRA-2 overestimates the amount of total AOD at all sites compared to AERONET by twice as much. Over the respective months evaluated at each site, for Tinga Tingana, the monthly mean AeroSpan/AERONET AOD was highest out of the sites at 0.0595 (550 nm)-0.066 (500 nm), its lowest monthly AOD over the period evaluated was 0.019 and highest recorded monthly AOD was 0.23. Birdsville had a total AOD monthly mean of 0.057 (500 nm)-0.055 (550 nm) with a range of 0.015-0.143 whereas with MERRA-2 (550 nm) AOD the mean was higher at 0.102 (range 0.049-0.216). Lake Lefroy had a similar mean AOD of 0.056 (500 nm)-0.058 (550 nm) with a range of 0.023-0.125 and again MERRA-2 grid at this site was twice as much at 0.093 total AOD (range, 0.046-0.216). Fowlers gap had the lowest AOD mean out of the sites 0.047 (500 nm)-0.053 (550 nm) with a

ACCEPTED MANUSCRIPT

412 range of 0.027-0.107 and at this site also MERRA-2 had higher total 550 nm AOD estimates

413 (mean, 0.096 and range 0.050-0.216).

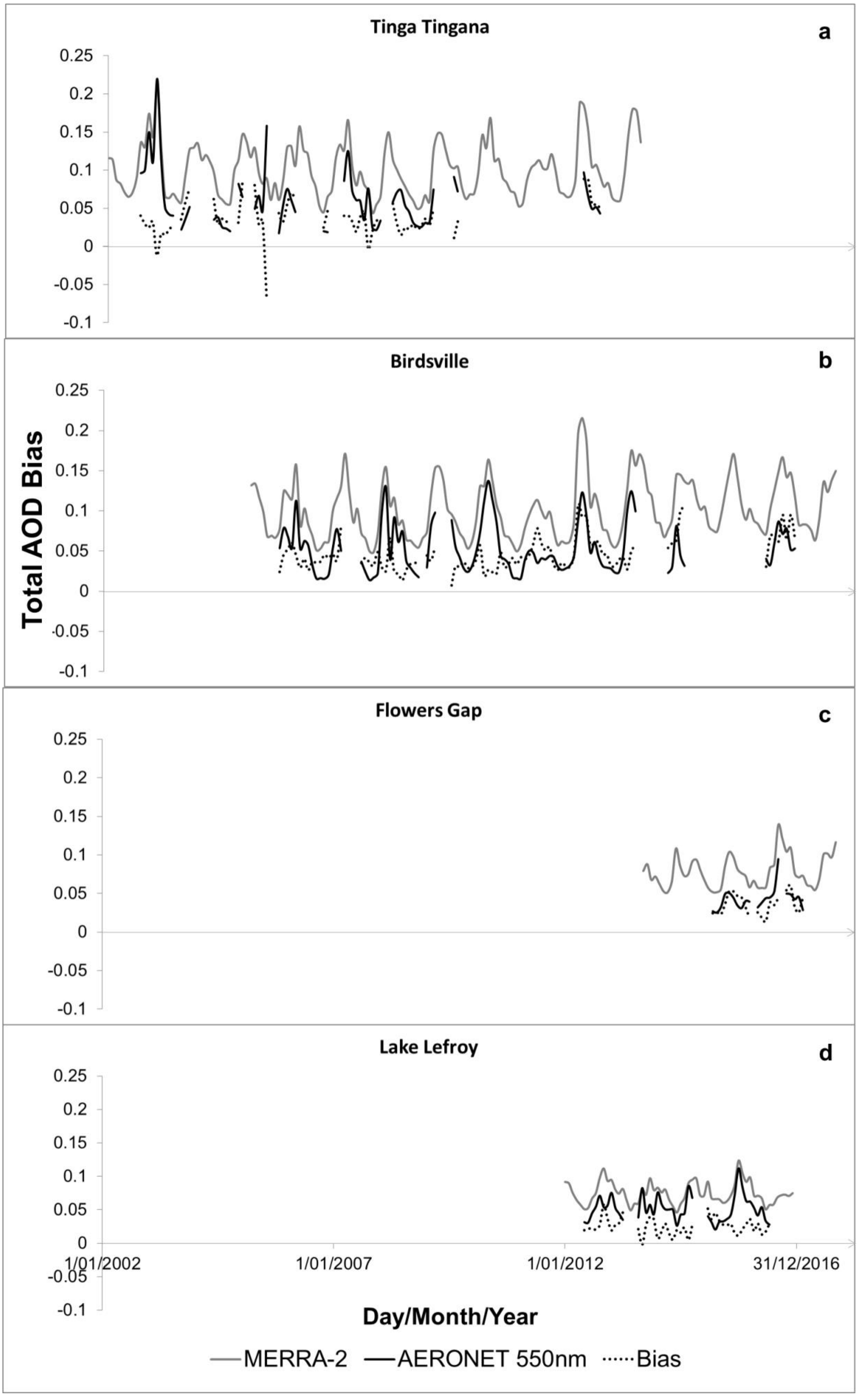

414

Figure 3. Monthly total AOD bias assessment between MERRA-2 and AERONET at 550 nm at: a. Tinga Tingana for 2002-2012 b. Birdsville 2005-2016 c. Flowers Gap 2013-2016 and d. Lake Lefroy 2012-2016

The time series plot in Fig. 4a shows large gaps in AeroSpan/AERONET daily mean total AOD observations with the level 2 dataset at Tinga Tingana for the years 2003 to 2012. The AOD values are low to moderate and the highest observed peak was at 0.71 (minimum 0.006 and mean 0.06 at 500 nm and 0.052 at 550 nm). The scatter plots in Fig. 4b-c are comparisons against the dust AOD between the reanalysis products against AERONET.

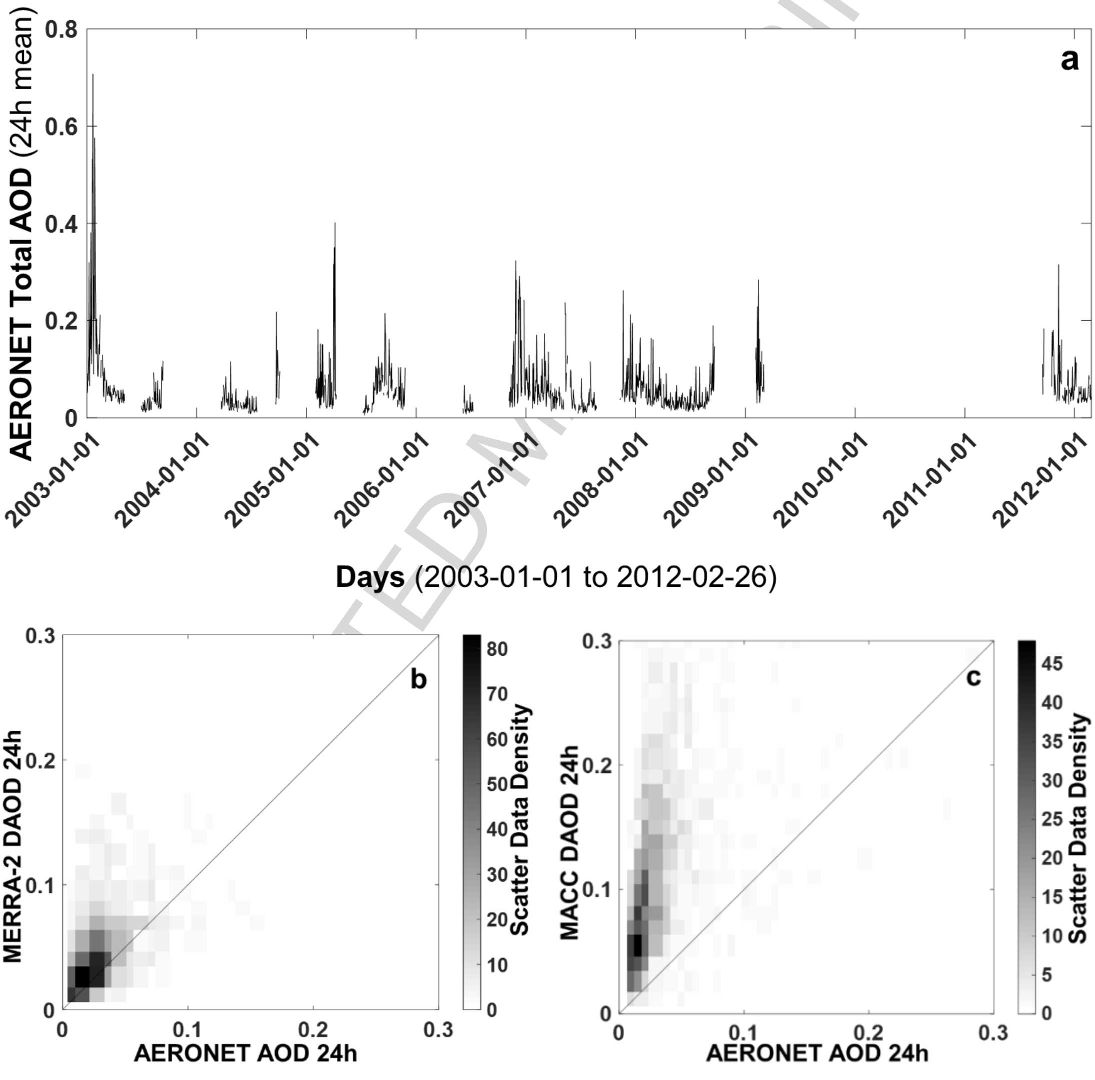

ACCEPTED MANUSCRIPT

ACCEPTED MANUSCRIPT

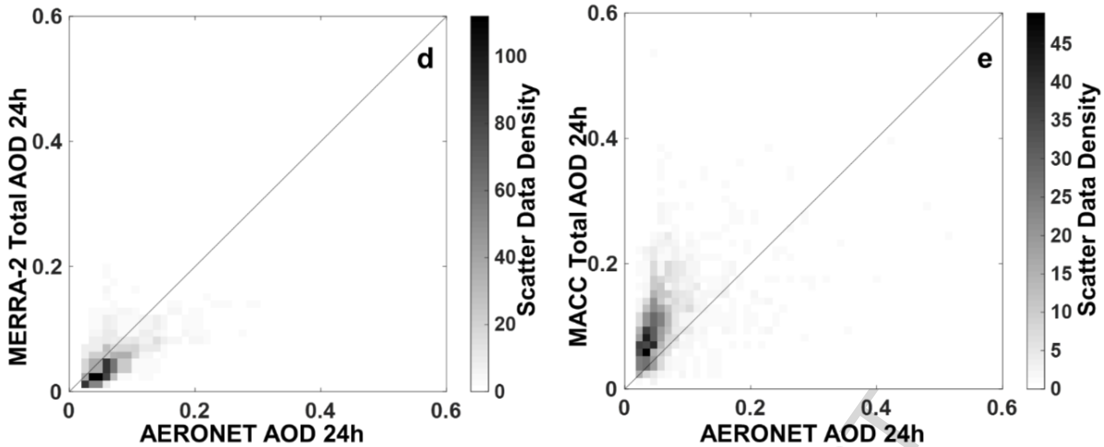

Figure 4. At Tinga Tingana: a. AERONET Total AOD (24h mean) (2003-01-01 to 2012-12-31) b. MERRA-2 dust extinction vs. AeroSpan/AERONET total AOD (2003-01-01 to 2012-02-26), with Pearson correlation (R = 0.46) c. same as b except for ECMWF/MACC dust AOD, (R = 0.44) d. same as b except MERRA-2 total AOD (R = 0.73) e. same as c except ECMWF/MACC total AOD (R =0.46)

Correlation between dust AOD of MERRA-2 and AERONET was R = 0.455 (Fig. 4b). The dust AOD correlation between MACC and AeroSpan/AERONET (Fig. 4c) was R = 0.437, which is slightly lower than between MERRA-2 and AeroSpan/AERONET. MERRA-2 total AOD correlation however, was much higher at 0.725 (Fig. 4d) against ground observations than MACC (R=0.463, Fig. 4e).

Table 3 outlines the differences between 550 nm and 500 nm based AeroSpan/AERONET estimates, for computed pearson correlation coefficient (R) and mean biases for the MERRA-2 and ECMWF/MACC datasets at Tinga Tingana. Using the angstrom exponent AOD estimate of 550 nm instead of 500 nm lowers the correlation significantly with MACC (R=0.213) and MERRA-2 (R=0.194) for dust AOD versus AeroSpan/AERONET AOD at Tinga Tingana. For total AOD as well, MACC (R=0.392) and MERRA-2 (R=0.586) were lower than with the original 500 nm dataset. The mean bias between MERRA-2 550 nm total AOD and AeroSpan/AERONET 500 nm total AOD was 0.02 (0.028 with 550 nm AeroSpan/AERONET) for the 24-hour mean datasets at Tinga Tingana. The mean bias of MERRA-2 dust AOD was -0.013 (550 nm) and -0.021 (500 nm). The bias for MACC total AOD was 0.049 (500 nm)-0.057 (550 nm). Thus, MACC total

ACCEPTED MANUSCRIPT

AOD is more biased than MERRA-2. MACC dust AOD of -9.1x10^{-5} (500 nm)-0.008 (550 nm) was less biased than MERRA-2 dust AOD compared to observations.

The mean angstrom exponent at Tinga Tingana was 0.8594 (range, -0.14-3.67). To reduce errors associated with angstrom based AOD approximation of 550 nm, we use the unmodified 500 nm dataset in the rest of this study to compare against 550 nm reanalysis datasets as it seems to be more accurate over the main site of interest, Tinga Tingana.

Table 3. Pearson correlation (R) and mean bias due to angstrom exponent based AeroSpan/AERONET AOD estimate for 550 nm and 500 nm with ECMWF/MACC and MERRA-2 total and dust AOD.

	550 nm AERONET		500 nm AERONET	
	MACC	MERRA-2	MACC	MERRA-2
R with Dust AOD	0.213	0.194	0.437	0.455
R with Total AOD	0.392	0.586	0.463	0.725
Mean bias with Dust AOD	0.008	-0.013	-9.10E-05	-0.021
Mean bias with Total AOD	0.057	0.028	0.049	0.02

The differences in correlation between the reanalysis datasets could be due to the variations in ECMWF/MACC and MERRA-2 model physics and assimilation schemes. For the computation of the trajectory forecast used in the ECMWF/MACC assimilation, the Integrated Forecast System (IFS) includes a number of tracers, which are advected by the model dynamics and interact with the various physical processes. With respect to the aerosols, sources are added to the model, and a representation of the aerosol physical processes is part of the package of physical parameterizations of the ECMWF IFS model. A prognostic representation of aerosols is a feature of numerous climate models (see, Textor et al. (2006), and Kinne et al. (2006) for reviews of how various aspects of aerosol physics are represented in recent general circulation models). However, it is more of a novelty in global weather forecast models, given the requirements on the assimilation system to deal properly with the aerosol-relevant observations and the time constraint for producing an analysis and subsequent forecast in a near-real-time environment. Aerosol-related observations (i.e., either aerosol optical depth retrievals or more directly, aerosol-sensitive radiances) are thus assimilated together with all the other observations in a fully interactive way (Benedetti et al., 2009).

The aerosol model contained in the ECMWF/MACC reanalysis (Morcrette et al., 2009) contains five aerosol types: sea salt (SS), desert dust (DD), organic matter (OM), black carbon (BC), and a sulfate-related variable (SU) at 550 nm. Sources of SS and DD are interactive and calculated with surface and near-surface variables of the model (Morcrette et al., 2008). The source function for the emission of desert dust is adapted from work by Ginoux et al. (2001), and is based on a limited number of climatological parameters (fraction of bare soil, vegetation cover, orography), some observations (MODIS component of UV-VIS surface albedo), and model prognostic variables (soil moisture, 10 m wind speed, snow cover, surface and top layer temperature). The aerosol assimilation scheme is part of the meteorological 4D-variational assimilation system employed operationally at ECMWF. The assimilation output, represents the best statistical compromise between the background information (i.e., the output of a short, 15 h forecast of the aerosol model) and the observations (Benedetti et al., 2009).

However, MERRA-2 includes an online implementation of the Goddard Chemistry, Aerosol, Radiation, and Transport model (GOCART) integrated into the Goddard Earth Observing System Model, Version 5 (GEOS-5) modeling system. GOCART simulates organic carbon, black carbon, sea salt, dust, and sulfate aerosols as well as sulfate aerosol precursors (dimethyl sulfide, sulfur dioxide), carbon monoxide and carbon dioxide. MERRA-2 has been extended to include assimilation of bias-corrected aerosol optical depth (AOD) from Advanced Very High Resolution Radiometer (AVHRR) and MODIS, Multi-angle Imaging SpectroRadiometer (MISR) AOD over bright surfaces, and AERONET AOD.

3.2 Direct comparison of reanalysis datasets (ECMWF/MACC vs. MERRA-2)

ACCEPTED MANUSCRIPT

In the case of direct comparisons between ECMWF/MACC and MERRA-2, the higher resolution ECMWF/MACC dataset was regridded to match the coarser MERRA-2 latitudes and longitudes.

First a daily time series over a decade long analysis was performed focusing on the Tinga Tingana site as an intercomparison between ECMWF/MACC and MERRA-2 to evaluate biases between the two datasets for total AOD. In Fig. 5a on the longer Tinga Tingana site time series of MERRA-2 total AOD 24h mean between 2002-01-01 to 2016-11-30 we overlaid the corresponding ECMWF/MACC 24h dataset from 2003-01-01 to 2012-12-31.

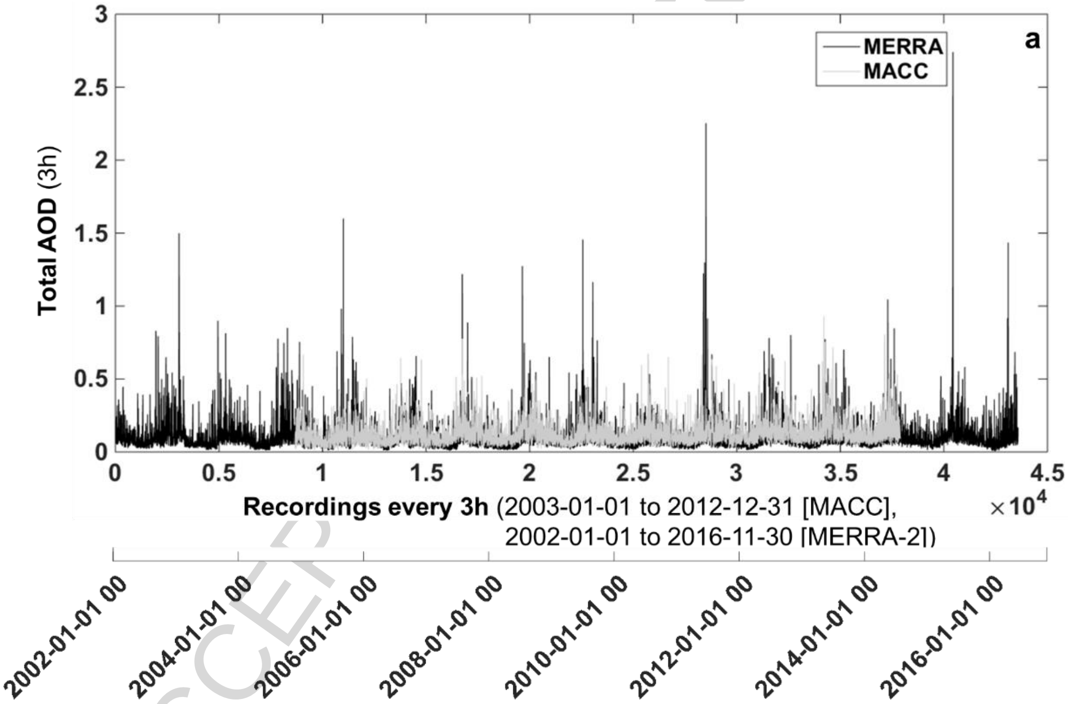

ACCEPTED MANUSCRIPT

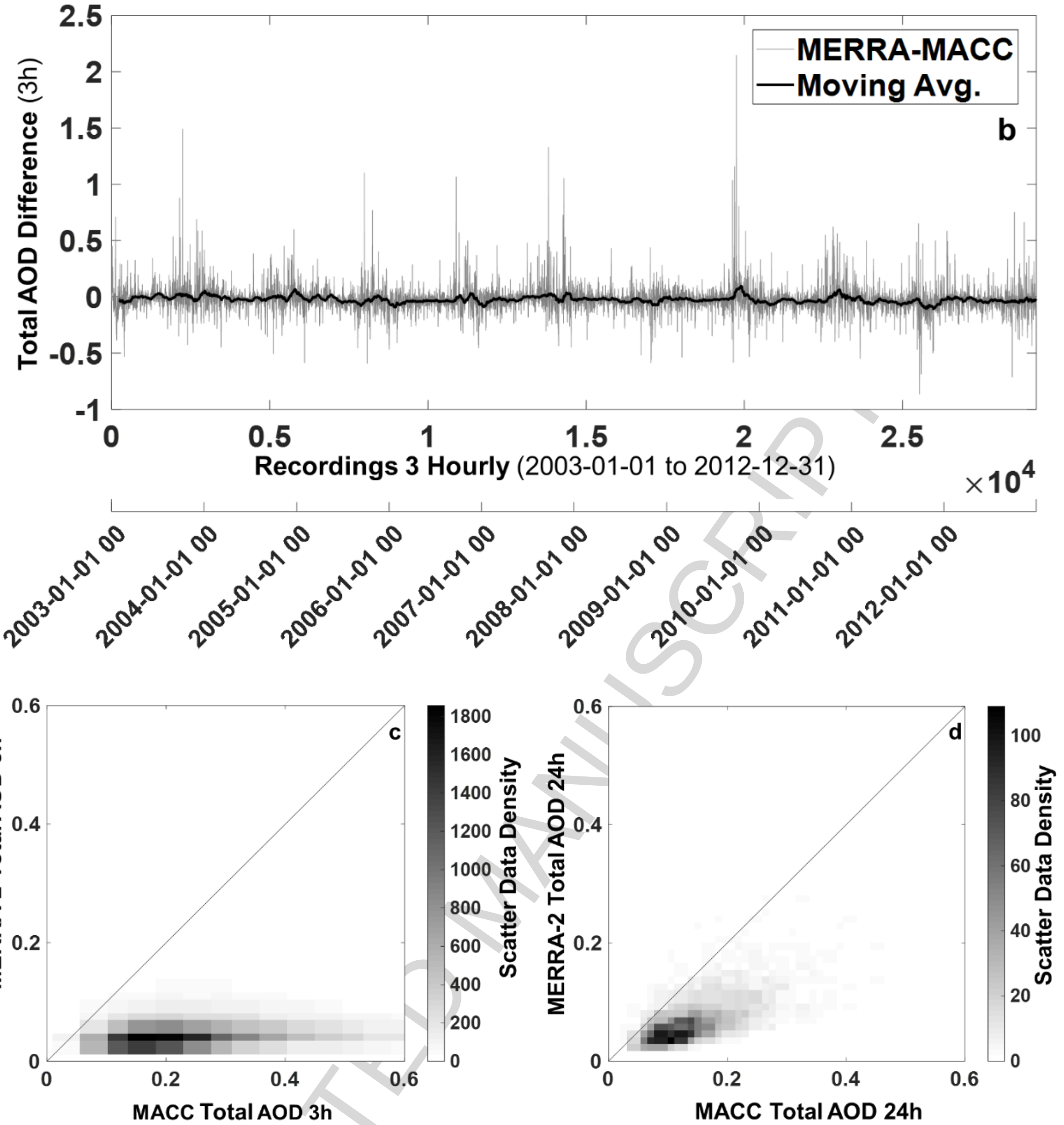

Figure 5. Time series at Tinga Tingana: a. of MERRA-2 Total AOD 3h (2002-01-01 to 2016-11-30) and ECMWF/MACC 3h (2003-01-01 to 2012-12-31) b. Difference between a) and b) 2003-01-01 to 2012-12-31 with 30-day moving average c. correlation at Tinga Tingana from scatter plot of MERRA AOD vs MACC AOD over 2003-01-01 to 2012-12-31 3 hourly with Pearson correlation (R = 0.4) d. Similar to c but daily average MACC and MERRA-2 (R=0.7)

Figure 5b shows significant differences between Fig. 5a MERRA and MACC Total AOD datasets for the period considered over the duration of ECMWF/MACC (2003-01-01 to 2012-12-31) during high AOD cases. The mean ECMWF/MACC 24-hour total AOD at Tinga Tingana was 0.12. This was a slightly higher estimate than the mean total AOD of MERRA-2 (over the time period of ECMWF/ MACC), at 0.097 and over the slightly longer period of MERRA-2 this was 0.098. MERRA-2 seems to provide higher total AOD estimates

ACCEPTED MANUSCRIPT

when the aerosols are high. However, looking at a 30-day moving average the differences between the two datasets do not seem significant and is close to zero.

These biases were further explored by evaluating correlations between the two datasets. The scatter plots in Fig. 5c are of three hourly recordings of MERRA AOD against MACC AOD over 2003-01-01 to 2012-12-31. The low correlation is obvious from the spread. However, when compared against the daily average in Fig. 5d, the correlation improves. This can be related to the increased stochasticity at shorter time frames but when averaged over an entire day, as the variability in the data is reduced, the MACC and ECMWF datasets are more representative of each other.

Furthermore, the dust aerosol optical depth was also analysed. Figure 6a shows both times series of MACC and MERRA-2 together. While the datasets tend to follow one another, exploring differences between the two reanalysis in Fig. 6b shows high differences in the dust AOD component again, particularly when the AOD's are high between the two reanalysis products similar to Fig 5b. MERRA-2 provides higher dust approximations during the extreme aerosol cases (AOD>1). In contrast, under normal cases for background AOD, looking at the 30-day moving average, the average difference was below zero indicating that MERRA-2 generally has lower dust AOD predictions than MACC. The range was much smaller in the case of dust AOD than total AOD comparing 5a-b with 6a-b. The mean dust AOD at Tinga Tingana from ECMWF/MACC was 0.06 and ranged from 0.006 to 0.347. For MERRA-2, mean dust AOD was 0.0467 (range, 0.004-0.468) and with the longer dataset around the same (0.0468).

ACCEPTED MANUSCRIPT

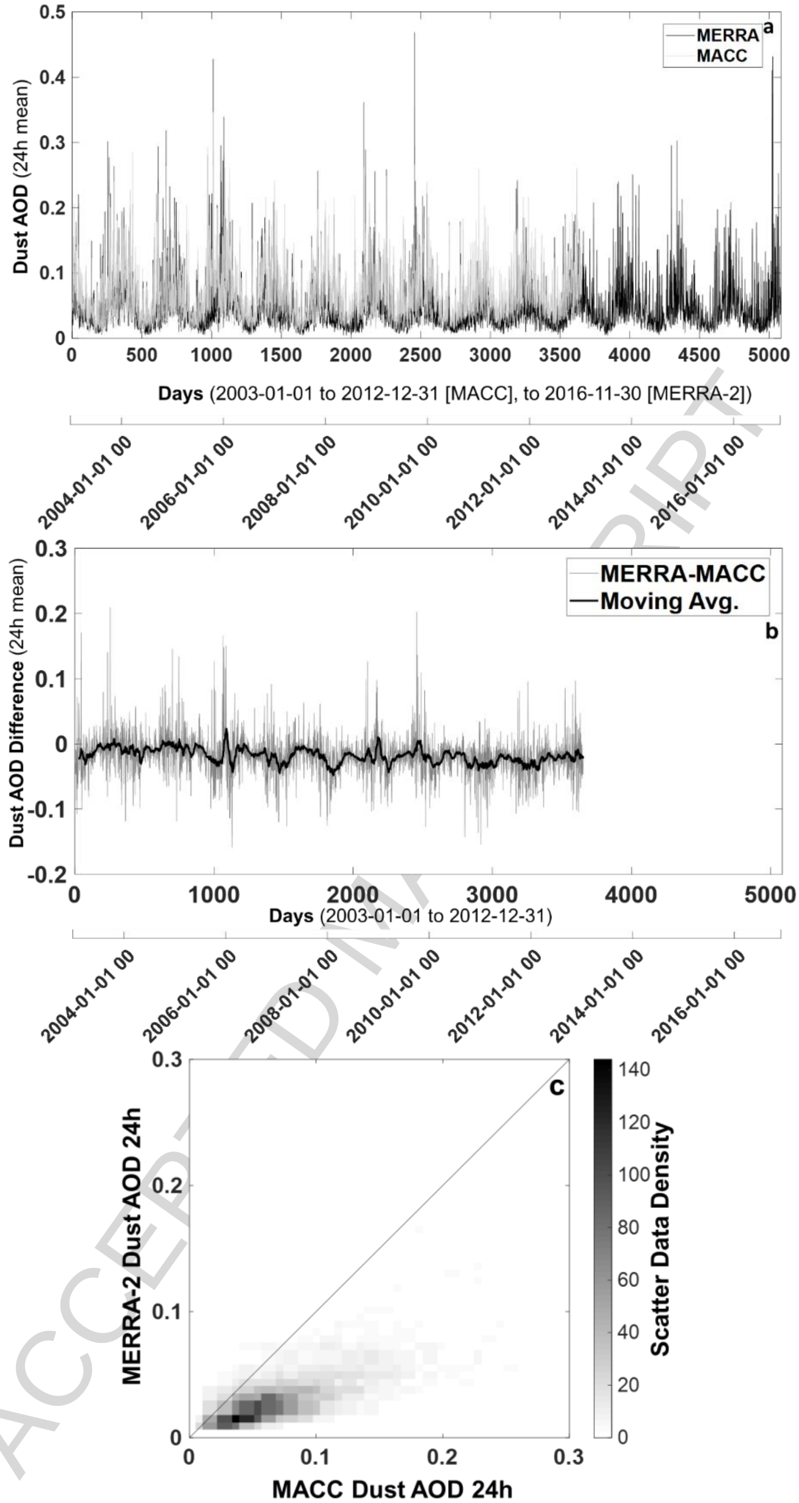

Figure 6. At Tinga Tingana: a. MERRA-2 (2003-01-01 to 2016-11-30) dust aerosol extinction and ECMWF/MACC (2003-01-01 to 2012-12-31) daily mean dust AOD 550 nm b. Difference between MERRA-2 and ECMWF/MACC in a with 30-dat moving average c. MERRA-2 vs MACC Dust AOD scatter plot of times series in a. with Pearson correlation, R = 0.73

The scatter plots in Fig. 6c are comparsions against the dust AOD between the reanalysis products. Between MERRA-2 dust AOD and MACC dust AOD (as in Fig. 6c) the correlation coefficient was R = 0.728. The dust AOD was only slightly higher than the total

ACCEPTED MANUSCRIPT

AOD correlation between MACC and MERRA-2 (R=0.697). Correlation between reanalysis dust datasets and AeroSpan/AERONET in section 3.1 above was much less ranging from R = 0.437 to 0.455. This correlation difference could be due to various reasons such as model resolution, model physics, chemical transport and assimilation limitations of current reanalysis, and cloud screening of dust in evaluating AeroSpan/AERONET AOD.

Next, we spatially assessed ECMWF/MACC and MERRA-2 datasets over the entire domain shown in Fig. 1 at each reanalysis grid point in Fig. 7a-c. The analysis shows both reanalysis datasets to be concentrated over Lake Eyre from Fig. 7a-c. From Fig. 7c however, we saw that MACC estimates dust AOD over the Lake Eyre Basin to be higher (by up to 40%) than MERRA-2 reanalysis over the five-year mean. In other regions with low dust AOD, MACC seems to provide lower dust estimates (shown in red) than MERRA-2 based on the difference between both reanalysis datasets in Fig. 7c.

ACCEPTED MANUSCRIPT

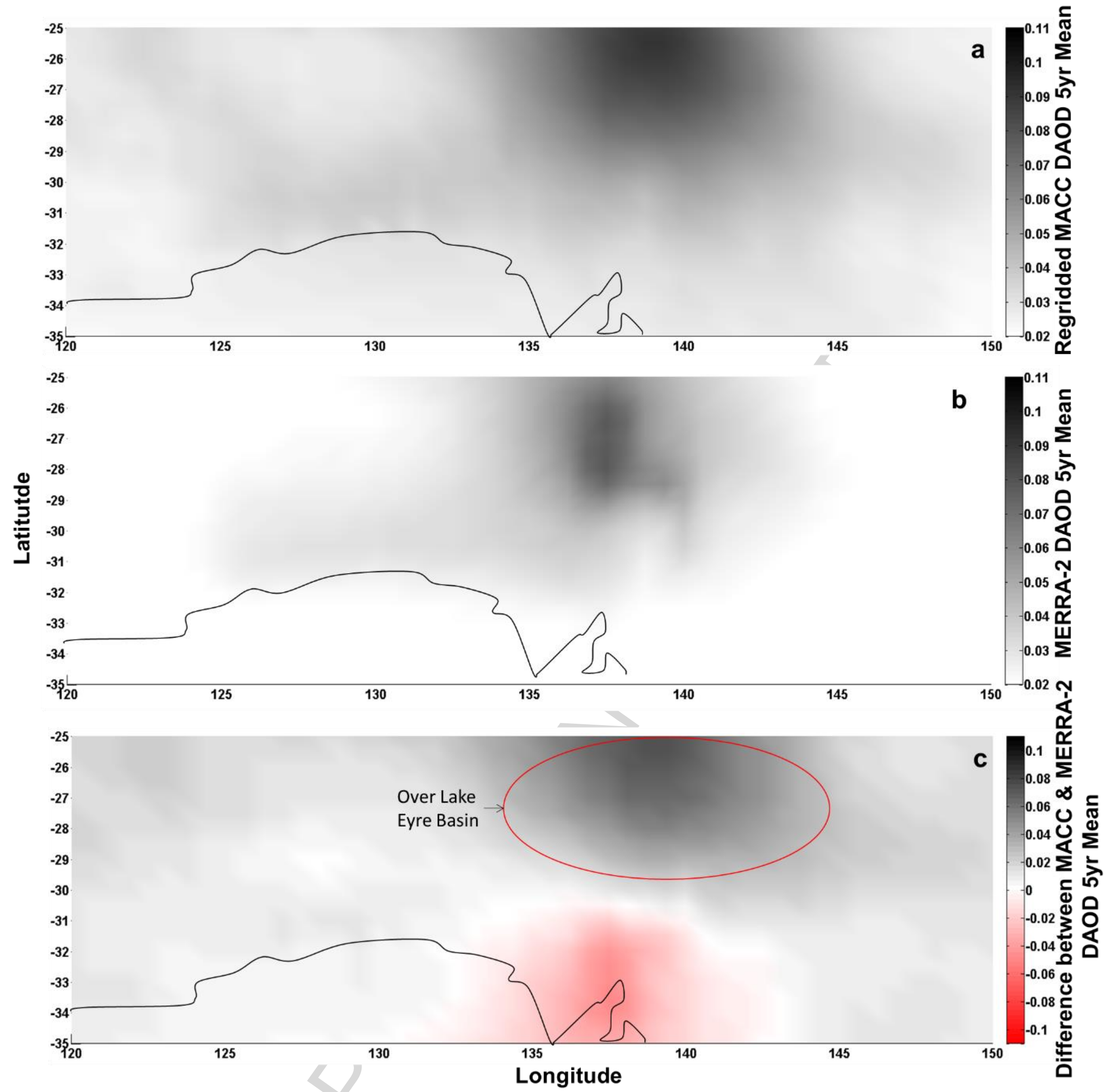

Figure 7. Spatial distribution of total AOD from reanalysis datasets over Australia between 2003 to 2008 a. ECMW/MACC at 0.125^{o} five year mean from 3 hourly data regridded to 0.5 x 0.625 (same as MERRA-2 resolution) b. MERRA-2 five-year mean from seasonal estimates c. Difference between a and b

3.3 Seasonal analysis

Beyond pointwise ground measurements and reanalysis intercomparisons in this study, the first analysis here involves a seasonal spatial comparison of MERRA-2 reanalysis area averaged over Australia for the domain shown in Fig 1 against the reference global study by Ridley et. al (2016). We use this reference study which relies on hybrid model estimates to check spatially averaged dust AOD estimates, because at present AERONET is too sparse to provide information about spatial or gridded distribution of aerosols around the Australian

ACCEPTED MANUSCRIPT

continent. While Ridley et al. (2016) estimates have an associated uncertainty; they are currently the best spatial estimate of dust AOD over Australia, especially when considering the entire range of hybrid estimates. The seasonal dust AOD of MERRA-2 mean gridded (Fig. 8a-d) is compared against Ridley et al., 2016 shown above in Table 2. The comparison against MERRA-2 is presented over the same time periods and seasons in 2003-2008 as Ridley et al. (2016).

In MERRA-2 the spatial distribution of dust AOD across the Australian continent varies comparing different seasons in Fig. 8a-d although they all are concentrated over the Lake Eyre Basin. The mean spatial variance and intensity of dust aerosol optical depth was highest in Sothern hemisphere summer (Dec, Jan & Feb or DJF for brevity from here on) 0.001-0.11 DAOD and lowest in Southern hemisphere winter 0.005-0.04 (June, July & Aug or JJA from here on). The spatial distribution of dust was most expansive in DJF followed by SON and MAM, the extent of dust distribution in JJA is very low.

A similar seasonal trend was observed visually in MERRA-2, see Fig. 8a-d to the Table 2 reference values. Thus MERRA-2 seasonal trend from our study which reveals the highest DAOD during summer (DJF), reduction over MAM, lowest over Winter (JJA), and increase from SON, is consistently comparable and validated against Ridley et al. (2016) reference models. The only exceptions to this trend are when their hybrid DOAD source + non-dust model have negative DAOD estimates. Our MERRA-2 results do not compare against their negative bias (explained in Section 2.3) because the reference study produces errors when other non-MERRAero sources (Terra, Aqua and MISR) are assimilated with a MERRAero model. However, validating MERRA-2 against MERRAero+MERRAero did not have the same issues since the hybrid reference MERRAero+MERRAero is well assimilated and did not have negative biases. The effects of seasonality can impact the results we see by affecting the correlation due to seasonal cycle which constitutes a more predictable component of the system. It is important to know how much of the correlation is due to the seasonal cycle,

ACCEPTED MANUSCRIPT

therefore it must be removed before computing the correlation. Thus, Fig. 9 shows the modified time series for reanalysis datasets ECMWF MACC, MERRA-2 and ground observations AeroSpan/AERONET at Tinga Tingana over a decade. The modified time series is a 91-day (approximate number of days per season) moving average using convolution of the original time series signals for reanalysis. The original daily dust AOD time series against AeroSpan/AERONET provided a correlation of 0.44 for MACC/ECMWF and 0.46 for MERRA-2 at Tinga Tingana whereas the modified time series (91-day moving average) gave an increased correlation of 0.56 for MACC/ECMWF and increased but lower correlation of 0.51 for MERRA-2.

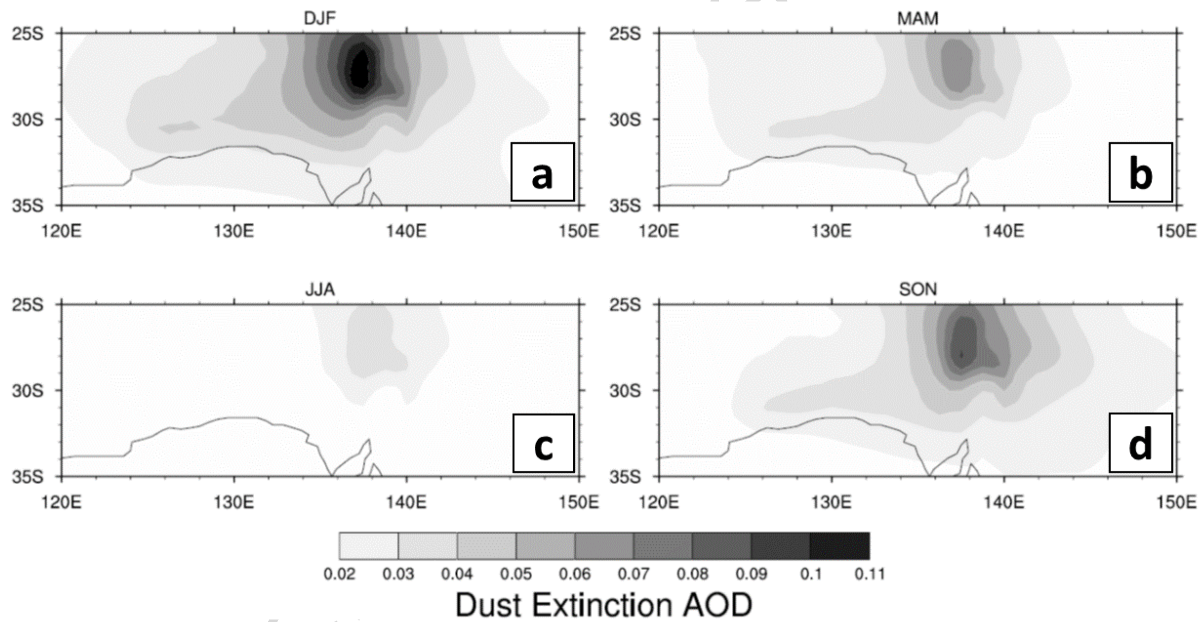

Figure 8. MERRA-2 gridded 0.5 x 0.625 degrees dust extinction aerosol optical depth (AOD) 550 nm monthly dataset seasonal mean from 2003-2008 over domain in Fig. 1 (35S, 120E to 25S, 150W) a. Dec, Jan, Feb 03-08 b. Mar, Apr, May 04-08 c. Jun, Jul, Aug 04-08 d. Sep, Oct, Nov 04-08. Seasons with missing months discarded.

ACCEPTED MANUSCRIPT

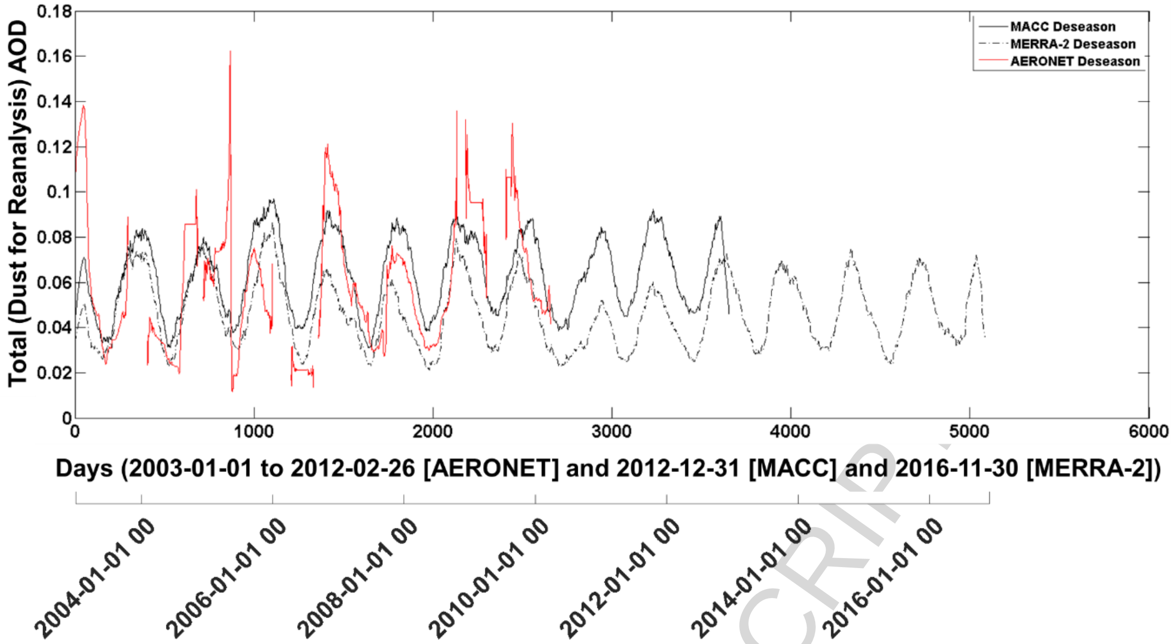

Figure 9. Reanalysis and AeroSpan/AERONET AOD modified time series (91-day moving average deseasonal) comparisons at Tinga Tingana

3.4 Detecting dust storms

Since the network is sparse over Australia, although one cannot expect AeroSpan/AERONET to provide information about transport, to explore suitability of detecting dust storms which are directly collocated, we analysed the daily average AOD data. The total AOD dataset showed large gaps in daily recordings in Fig. 4a and (reproduced overlaid with dust storm and AOD levels in) Fig. 10a below. Therefore, while AERONET Level 2 is suitable for monthly climatological assessments with slow changing background aerosol, it is not useful for dust storms at daily to sub-daily time scales even if the dust storm is co-located with the station, due to cloud screening. In Fig. 10a the Level 1.5 dataset without cloud screening seems to retain higher peaks which in some instances correspond with extreme dust events but the background AOD calculated is less accurate than Level 2. Around 6 peaks exceeding AOD 0.75 were identified in Level 1.5 whereas none were found in Level 2. To investigate the suitability for the reanalysis products to capture the dust storm events (e.g. for subsequent model assimilation in future studies), taking this analysis even further to a specific case study such as the 2009 Australian dust storm, we see that the reanalysis products show high total AOD (Fig. 10b) peaks which are clearly visible from the

ACCEPTED MANUSCRIPT

3 hourly datasets. MERRA-2 seems to provide higher dust AOD estimates than ECMWF/MACC reanalysis product during dust storms but when averaged over the day it provides lower AOD estimates as we found even in the yearly average comparisons in Fig. 5d over Lake Eyre basin.

AeroSpan/AERONET Level 2 does not offer any useful information about the event from the low daily total AOD (Fig. 10c) and also when we explored the sub-daily raw data (outside what is shown in this study). Thus, from Figure 10 during the 2009 Australian dust storm it was apparent that the dust AOD cannot be detected by AERONET due to missing datasets and limitations in sun photometry.

Based on our analysis in Sections 3.1-3.3, reanalysis datasets of dust AOD at monthly, daily and even three-hourly resolution, did not provide sufficient information to detect dust storms. The daily MERRA-2 datasets analysed earlier only ranged from 0.004 to 0.468 and MACC ranged from 0.006 to 0.347, thus they have insufficient temporal resolution to detect extreme events (defined here as 0.75>AOD). Using the three hourly MACC dataset the AOD range was between 0.004 to 0.728. At present, even MACC 3 hourly dataset seems unsuitable for detecting extreme events over Australia. Therefore, if reanalysis datasets must be used to detect dust storms over Australia, this study shows that the highest temporal resolution available (up to hourly from MERRA-2) must be analysed. Figure 10d thus shows the highest resolution of 1 hour from MERRA-2. Here we observe that, the dust AOD ranges from 0.001 to 1.503. Using the higher resolution MERRA-2, around nine extreme aerosol events were detected including the extreme 2009 Australian dust storm.

And finally, since AeroSpan/AERONET Level 2 cloud screens major dust storms, we also qualitatively verify reanalysis estimates against a continuously operating nephelometer using data recording during the 2009 Australian Dust Storm event as a case study. The nephelometer datasets show high scattering during the dust event from 21-09-09 UTC onwards, which coincides with the high dust AOD estimates of the reanalysis products. The scattering coefficient (mM^{-1}) before the peak of the event 20th Sep 8 UTC to 21st Sep 8 UTC was quite low (up to 100mM^{-1}). There was high scatter (up to 5000mM^{-1}) due to the dust storm from 21st Sep 12 UTC to 22nd Sep 12 UTC. Mitchell et al. (2010), showed that the background scattering coefficient at Tinga Tingana was σ_{sca} ~10 Mm^{-1}, with significantly elevated levels above that, as also identified in this study, corresponding to dust mobilization. Mitchell et al. (2010) quantified the relationship between nephelometer signal and dust mobilization, referring to events with $100 < \sigma_{sca} < 1000$ Mm^{-1} as 'significant' events, and those with σ_{sca} greater than 1000 Mm^{-1} as 'major' events. Thus, analysing the extreme 2009 Australian dust storm event nephelometer data peaks in this study is consistent with Mitchell et al. (2010) event definitions. Moreover, this adds weight to the central assumption inherent in Mitchell et al. (2010), O'Loingsigh et al. (2015a), and ours - that dust measured at Tinga Tingana can be used to characterize dust mobilisation over the Strzelecki Lakes. Future work for dust storm analysis could consider integrated nephelometer assessments with AeroSpan/AERONET, high resolution reanalysis and satellite observations.

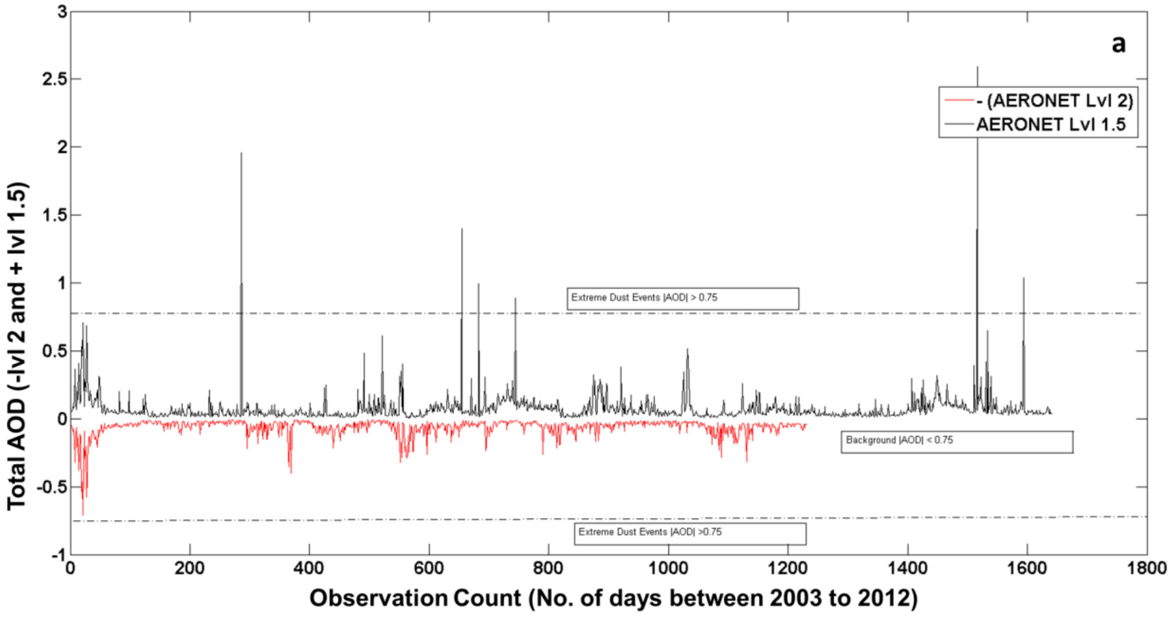

ACCEPTED MANUSCRIPT

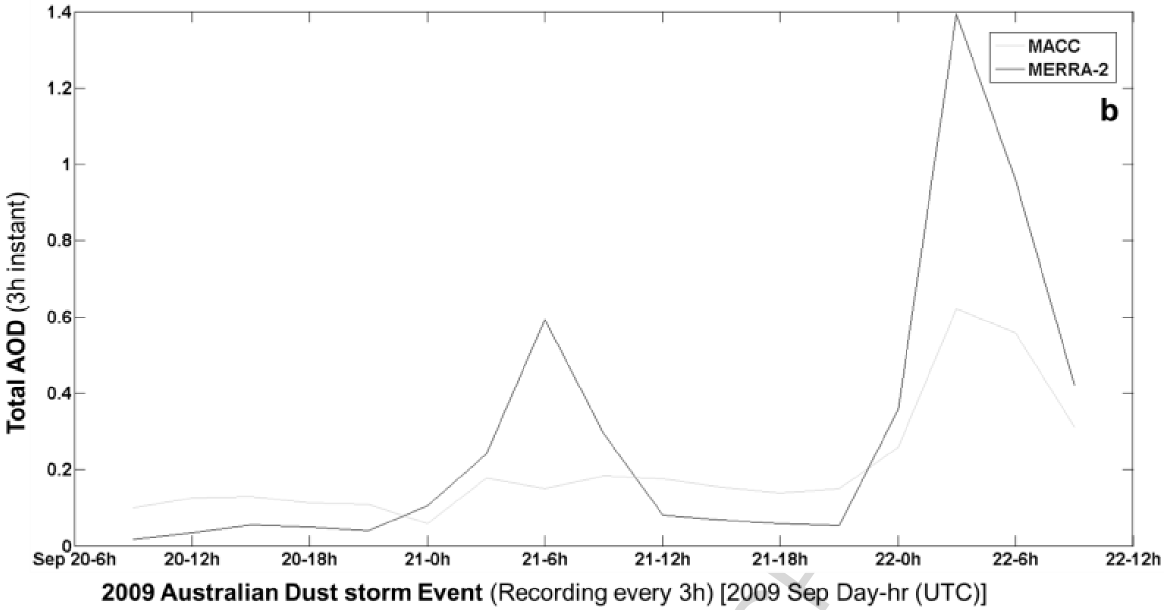

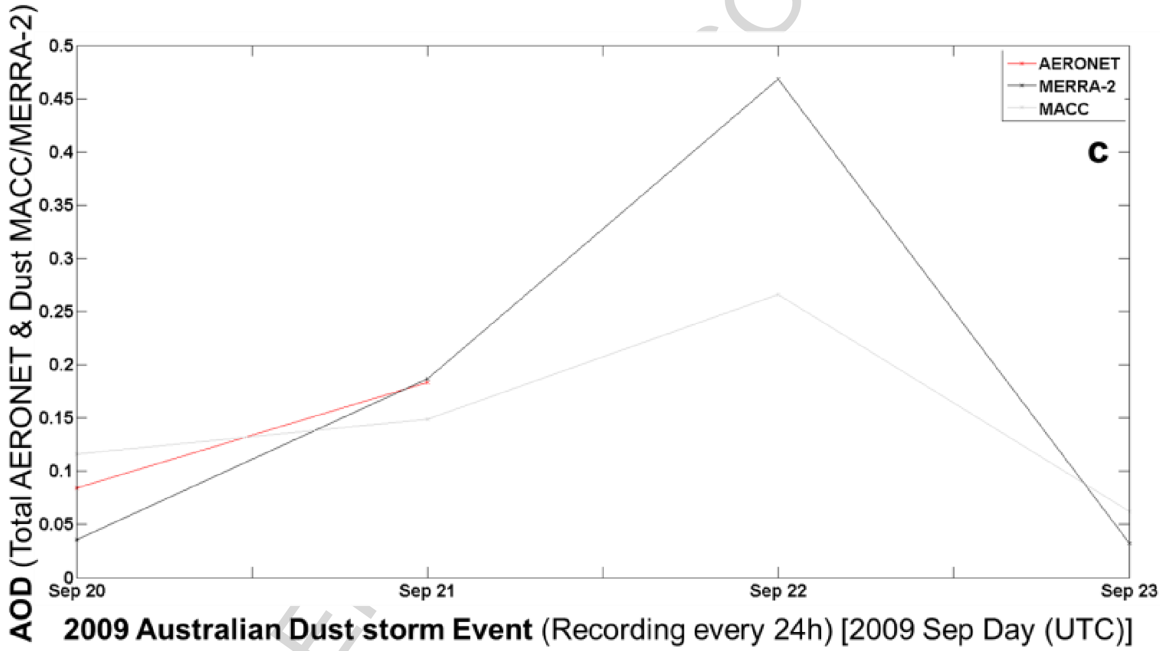

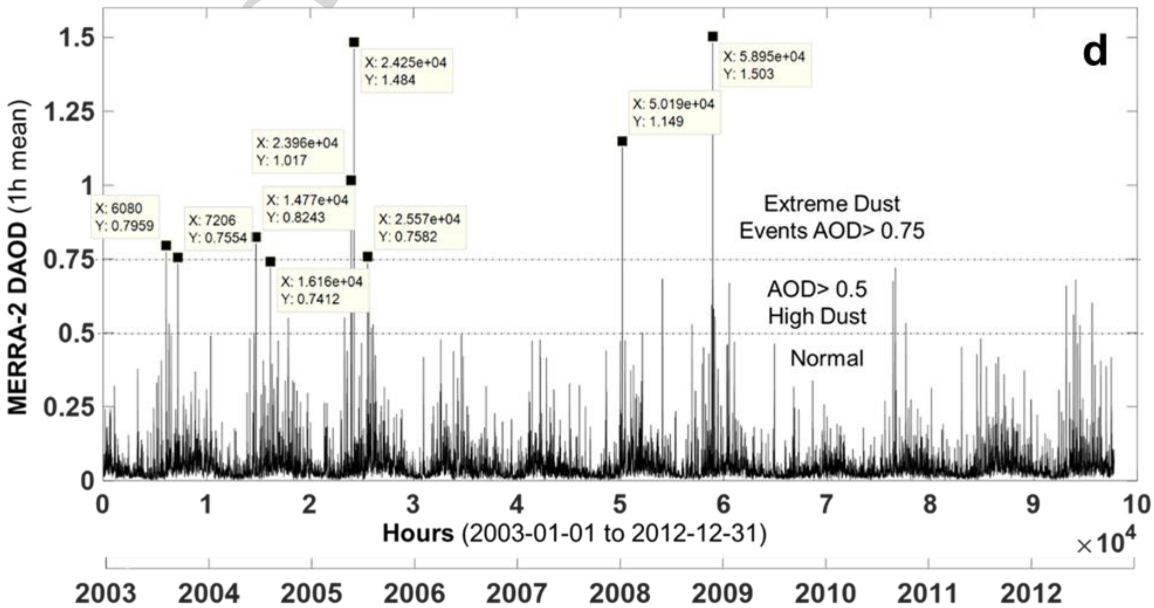

Figure 10. Total AOD and Dust AOD (DAOD) at Tinga Tingana – comparison between long term record and 2009 dust storm event: a. AeroSpan/AERONET data Version 2.0 Level 1.5 and Level 2, 24 hour mean observation count over the period 2003-01-01 to 2012-02-26 b. MERRA-2 and MACC (3h inst) Total AOD 550 nm during Australian dust storm during 2009-09-20:9h UTC to 2009-09-22:9h UTC where y- axis: Total AOD (3h instantaneous); x-axis: 3 hourly time recordings (between Sep 20th at 6 UTC to Sep 22nd at 12 UTC) c. Daily mean for ECMWF/MACC and MERRA-2 AOD 2009-09-20 to 2009-09-23 including AeroSpan/AERONET recordings where y-axis: Total AOD (24h mean); x-axis: Day of the month (Sep 20th to Sep 23rd). d. MERRA-2 1 hour dust AOD shows extreme events

4. Conclusions

In this study, atmospheric total and dust aerosol optical depth (AOD) from reanalysis datasets were analysed over Australia. The first objective of this study was to assess aerosol reanalysis against ground measurements. We studied the decadal aerosol reanalysis over Australia, focusing on key dust activation AERONET/AeroSpan site Tinga Tingana in the Lake Eyre basin. This analysis showed that the correlation between MERRA-2 dust AOD and AeroSpan/AERONET total AOD was low and comparable to ECMWF/MACC. However, MERRA-2 total AOD had much higher correlation against AeroSpan/AERONET total AOD than ECMWF/MACC. Differences between the reanalysis dataset assimilation inputs and model resolution were discussed which may contribute to different estimates between ECMWF/MACC and MERRA-2 over Australia. Time series revealed MERRA-2 to be generally positively biased compared to AeroSpan/AERONET at all sites. Large gaps were found in AeroSpan/AERONET datasets and limited observation sites at high resolutions to validate reanalysis with high confidence over the entire Australian continent. While both ECMWF/MACC and MERRA-2 provided dust estimates during normal conditions and an extreme event, the MERRA-2 seems to be more sensitive with higher dust estimates during extreme events. Spatial analysis over a new domain based on Ridley et al. (2016), showed ECMWF/MACC had up to 40% higher AOD over the Lake Eyre Basin than MERRA-2 from annual averages. In MERRA-2 the spatial distribution of dust AOD across Australia varies with seasons although they are all concentrated over the Lake Eyre Basin. The spatial

ACCEPTED MANUSCRIPT

distribution of dust is most expansive in summer and the extent of dust distribution in winter was very low.

In addition, our study extends Ridley et al. (2016) and other literature by further investigating detection of extreme dust events over Australia using observations and reanalysis. The study linked nephelometer comparisons during the 2009 Australian dust storm with AOD. Differences between level 1.5 and level 2 products were found, which showed that level 1.5 without cloud screening might be more suitable for dust storm detection than level 2. From the higher temporal resolution MERRA-2 1 hourly reanalysis, up to 11 extreme dust events were detected providing further insight about temporal resolution of dust storms in reanalysis datasets. Overall, this study highlights that high-resolution reanalysis datasets (e.g. MERRA-2) must be considered in addition to AeroSpan/AERONET level 1.5 unscreened data to help improve the simulation (i.e. reconstruction) of aerosols with numerical weather prediction models (also used for reanalyses) over Australia along with nephelometer signals.

Acknowledgements

The authors would like to thank David A. Ridley at MIT for useful contributions, feedback and data from their manuscript (Ridley et al., 2016) of dust aerosol optical depth (AOD) observationally constrained hybrid satellite and model output estimates over Australia from their global study. Thanks also extend to AERONET managed by project leader Brent N. Holben in conjunction with CSIRO's AeroSpan network for AOD and nephelometer data, NASA Global Modelling and Assimilation Office (GMAO) Goddard Earth Sciences Data Information Services Center (GES DISC) for MERRA-2 product, ECMWF MACC II Products and Consortium for AOD reanalysis. This research did not receive any specific grant from funding agencies in the public, commercial, or not-for-profit sectors.

ACCEPTED MANUSCRIPT

ACCEPTED MANUSCRIPT

This publication is dedicated to Dr Ross Mitchell, who established the AeroSpan network to monitor and characterise the continental dust and smoke aerosols that affect Australia's climate.

Source	**Type**	**Variable**	**Frequency**	**Period**	**Domain/Site**
Ridley et al. (2016) MIT-UCLA-PNNL study	16 Hybrid dust source + non-dust spatial average Monte Carlo model outputs	DAOD 550nm	Seasonal mean	2003 Dec-2008 Nov	(35S, 120E to 20S, 150W)
MERRA-2 (GMAO, 2015a, 2015b, 2015c)	Gridded Reanalysis $0.5^{o}x0.625^{o}$	DAOD 550nm	Monthly mean	2003-2008	(35S, 120E to 25S, 150W)
		Total AOD 550nm	3 hourly instant	2003-2008	(35S, 120E to 25S, 150W)
	Reanalysis grid point $0.5^{o}x0.625^{o}$ closest to AeroSpan/AERONET site	Total AOD 550nm	Monthly mean	2002-2012	Tinga Tingana
				2005-2016	Birdsville
				2013-2016	Flowers Gap
				2012-2016	Lake Lefroy
		Total AOD 550nm	24h mean	2002-01-01 to 2016-11-30	Tinga Tingana
			3 hourly instant	2002-01-01 to 2016-11-30	Tinga Tingana
ECMWF/ MACC (Inness et al., 2013b)	Gridded Reanalysis 0.125^{o}	DAOD 550 nm	3 hourly instant	2003-2008	(35S, 120E to 25S, 150W)
	Reanalysis grid point 0.125^{o}	DAOD 550 nm	3 hourly instant	2003-2012	Tinga Tingana
		Total AOD 550 nm	3 hourly instant	2003-2012	Tinga Tingana
AeroSpan/ AERONET v2 (2018) (Holben et al., 1998)	Aerosol Observations	Total AOD 500 nm	Monthly mean	2002-2012	Tinga Tingana
				2005-2016	Birdsville
				2013-2016	Flowers Gap
				2012-2016	Lake Lefroy
		Total AOD 500nm	24h mean	2002-2012	Tinga Tingana
	Nephelometer (2009 Australian dust storm event)	Scattering Coefficient (Mm^{-1})	Continuous	Sep 21- Sep 22 2009	Tinga Tingana

ACCEPTED MANUSCRIPT

Sources + Model	DJF	MAM	JJA	SON
Aqua+GeosChem	0.0344	0.0173	0.0020	0.0148
Aqua+CESM	0.0446	0.0139	0.0000	0.0159
Aqua+WRFChem	0.0428	0.0149	-0.0061	0.0151
Aqua+MERRAero	-0.0020	-0.0076	-0.0212	-0.0438
Terra+GeosChem	0.0292	0.0192	0.0078	0.0077
Terra+CESM	0.0375	0.0176	0.0061	0.0075
Terra+WRFChem	0.0375	0.0172	-0.0007	0.0082
Terra+MERRAero	-0.0102	-0.0057	-0.0155	-0.0533
Misr+GeosChem	0.0342	0.0144	-0.0018	0.0247
Misr+CESM	0.0423	0.0108	-0.0040	0.0249
Misr+WRFChem	0.0422	0.0137	-0.0087	0.0255
Misr+MERRAero	-0.0035	-0.0098	-0.0244	-0.0356
GeosChem+GeosChem	0.0448	0.0248	0.0172	0.0498
CESM+CESM	0.0748	0.0302	0.0064	0.0636
WRFChem+WRFChem	0.0345	0.0270	0.0201	0.0335
MERRAero+MERRAero	0.0419	0.0330	0.0202	0.0351

ACCEPTED MANUSCRIPT

	550 nm AERONET		500 nm AERONET	
	MACC	MERRA-2	MACC	MERRA-2
R with Dust AOD	0.213	0.194	0.437	0.455
R with Total AOD	0.392	0.586	0.463	0.725
Mean bias with Dust AOD	0.008	-0.013	-9.10E-05	-0.021
Mean bias with Total AOD	0.057	0.028	0.049	0.02

References

[dataset] AeroSpan/AERONET v2, 2018. Aerosol characterisation via Sun photometry: Australian network (AeroSpan)/Aerosol Robotic Network version 2. https://aeronet.gsfc.nasa.gov/cgi-bin/webtool_opera_v2_new?stage=2&place_code=10&region=Australia_and_Pacific&state=Australia&submit=Get+AERONET+Sites (accessed 6 Feb 2018)

Alexandri, G., Georgoulias, A.K., Meleti, C., Balis, D., Kourtidis, K.A., Sanchez-Lorenzo, A., Trentmann, J., Zanis, P., 2017. A high resolution satellite view of surface solar radiation over the climatically sensitive region of Eastern Mediterranean. Atmos. Res. https://doi.org/https://doi.org/10.1016/j.atmosres.2016.12.015

Beegum, S.N., Gherboudj, I., Chaouch, N., Temimi, M., Ghedira, H., 2018. Simulation and analysis of synoptic scale dust storms over the Arabian Peninsula. Atmos. Res. https://doi.org/https://doi.org/10.1016/j.atmosres.2017.09.003

Benedetti, A., Morcrette, J.-J., Boucher, O., Dethof, A., Engelen, R.J., Fisher, M., Flentje, H., Huneeus, N., Jones, L., Kaiser, J.W., Kinne, S., Mangold, A., Razinger, M., Simmons, A.J., Suttie, M., 2009. Aerosol analysis and forecast in the European Centre for Medium-Range Weather Forecasts Integrated Forecast System: 2. Data assimilation. J. Geophys. Res. Atmos. 114, n/a-n/a. https://doi.org/10.1029/2008JD011115

Boucher, O., Randall, D., Artaxo, P., Bretherton, C., Feingold, G., Forster, P., Kerminen, V.-M., Kondo, Y., Liao, H., Lohmann, U., 2013. Clouds and aerosols, Climate change 2013: the physical science basis. Contribution of Working Group I to the Fifth Assessment Report of the Intergovernmental Panel on Climate Change. Cambridge University Press.

Boyd, P.W., McTainsh, G., Sherlock, V., Richardson, K., Nichol, S., Ellwood, M., Frew, R., 2004. Episodic enhancement of phytoplankton stocks in New Zealand subantarctic waters: Contribution of atmospheric and oceanic iron supply. Global Biogeochem. Cycles 18, n/a-n/a. https://doi.org/10.1029/2002GB002020

Buchard, V., Randles, C.A., da Silva, A.M., Darmenov, A., Colarco, P.R., Govindaraju, R., Ferrare, R., Hair, J., Beyersdorf, A.J., Ziemba, L.D., Yu, H., 2017. The MERRA-2 Aerosol Reanalysis, 1980 Onward. Part II: Evaluation and Case Studies. J. Clim. 30, 6851–6872. https://doi.org/10.1175/JCLI-D-16-0613.1

ACCEPTED MANUSCRIPT

Bullard, J., Baddock, M., McTainsh, G., Leys, J., 2008. Sub-basin scale dust source geomorphology detected using MODIS. Geophys. Res. Lett. 35, n/a-n/a. https://doi.org/10.1029/2008GL033928

Chan, Y.-C., Mctainsh, G., Leys, J., Mcgowan, H., Tews, K., 2005. Influence of the 23 October 2002 dust storm on the air quality of four Australian cities. Water. Air. Soil Pollut. 164, 329–348.

Choobari, O.A., Zawar-Reza, P., Sturman, A., 2014. The global distribution of mineral dust and its impacts on the climate system: A review. Atmos. Res. https://doi.org/https://doi.org/10.1016/j.atmosres.2013.11.007

Dubovik, O., Sinyuk, A., Lapyonok, T., Holben, B.N., Mishchenko, M., Yang, P., Eck, T.F., Volten, H., Muñoz, O., Veihelmann, B., van der Zande, W.J., Leon, J.-F., Sorokin, M., Slutsker, I., 2006. Application of spheroid models to account for aerosol particle nonsphericity in remote sensing of desert dust. J. Geophys. Res. Atmos. 111, n/a-n/a. https://doi.org/10.1029/2005JD006619

Evans, S., Ginoux, P., Malyshev, S., Shevliakova, E., 2016. Climate-vegetation interaction and amplification of Australian dust variability. Geophys. Res. Lett. 43, 11,811-823,830. https://doi.org/10.1002/2016GL071016

Gabric, A.J., Cropp, R.A., McTainsh, G.H., Johnston, B.M., Butler, H., Tilbrook, B., Keywood, M., 2010. Australian dust storms in 2002–2003 and their impact on Southern Ocean biogeochemistry. Global Biogeochem. Cycles 24, n/a-n/a. https://doi.org/10.1029/2009GB003541

Gelaro, R., McCarty, W., Suárez, M.J., Todling, R., Molod, A., Takacs, L., Randles, C.A., Darmenov, A., Bosilovich, M.G., Reichle, R., Wargan, K., Coy, L., Cullather, R., Draper, C., Akella, S., Buchard, V., Conaty, A., da Silva, A.M., Gu, W., Kim, G.-K., Koster, R., Lucchesi, R., Merkova, D., Nielsen, J.E., Partyka, G., Pawson, S., Putman, W., Rienecker, M., Schubert, S.D., Sienkiewicz, M., Zhao, B., 2017. The Modern-Era Retrospective Analysis for Research and Applications, Version 2 (MERRA-2). J. Clim. 30, 5419–5454. https://doi.org/10.1175/JCLI-D-16-0758.1

Gillingham, S.S., Flood, N., Gill, T.K., Mitchell, R.M., 2012. Limitations of the dense dark vegetation method for aerosol retrieval under Australian conditions. Remote Sens. Lett. 3, 67–76. https://doi.org/10.1080/01431161.2010.533298

Ginoux, P., Chin, M., Tegen, I., Prospero, J.M., Holben, B., Dubovik, O., Lin, S.-J., 2001. Sources and distributions of dust aerosols simulated with the GOCART model. J. Geophys. Res. Atmos. 106, 20255–20273. https://doi.org/10.1029/2000JD000053

[dataset] Global Modeling and Assimilation Office (GMAO), 2015a. MERRA-2 tavgM_2d_aer_Nx: 2d,Monthly mean,Time-averaged,Single-Level,Assimilation,Aerosol Diagnostics V5.12.4, Greenbelt, MD, USA, Goddard Earth Sciences Data and Information Services Center (GES DISC), (accessed 6 Feb 2018) https://doi.org/10.5067/FH9A0MLJPC7N

[dataset] Global Modeling and Assimilation Office (GMAO), 2015b, MERRA-2 inst3_2d_gas_Nx: 2d,3-Hourly,Instantaneous,Single-Level,Assimilation,Aerosol Optical Depth Analysis V5.12.4, Greenbelt, MD, USA, Goddard Earth Sciences Data and

Information Services Center (GES DISC), Accessed (accessed 6 Feb 2018) 10.5067/HNGA0EWW0R09

[dataset] Global Modeling and Assimilation Office (GMAO), 2015c, MERRA-2 tavg1_2d_aer_Nx: 2d,1-Hourly,Time-averaged,Single-Level,Assimilation,Aerosol Diagnostics V5.12.4, Greenbelt, MD, USA, Goddard Earth Sciences Data and Information Services Center (GES DISC), Accessed (accessed 6 Feb 2018) https://doi.org/10.5067/KLICLTZ8EM9D

Goudie, A.S., Middleton, N.J., 1992. The changing frequency of dust storms through time. Clim. Change 20, 197–225.

Gras, J.L., Ayers, G.P., 1983. Marine aerosol at southern mid-latitudes. J. Geophys. Res. Ocean. 88, 10661–10666. https://doi.org/10.1029/JC088iC15p10661

Gras, J.L., 1991. Southern hemisphere tropospheric aerosol microphysics. J. Geophys. Res. Atmos. 96, 5345–5356. https://doi.org/10.1029/89JD00429

Heald, C.L., Ridley, D.A., Kroll, J.H., Barrett, S.R.H., Cady-Pereira, K.E., Alvarado, M.J., Holmes, C.D., 2014. Contrasting the direct radiative effect and direct radiative forcing of aerosols. Atmos. Chem. Phys. 14, 5513–5527.

Holben, B.N., Eck, T.F., Slutsker, I., Tanré, D., Buis, J.P., Setzer, A., Vermote, E., Reagan, J.A., Kaufman, Y.J., Nakajima, T., Lavenu, F., Jankowiak, I., Smirnov, A., 1998. AERONET—A Federated Instrument Network and Data Archive for Aerosol Characterization. Remote Sens. Environ. https://doi.org/https://doi.org/10.1016/S0034-4257(98)00031-5

Hollingsworth, A., Engelen, R.J., Benedetti, A., Dethof, A., Flemming, J., Kaiser, J.W., Morcrette, J.-J., Simmons, A.J., Textor, C., Boucher, O., Chevallier, F., Rayner, P., Elbern, H., Eskes, H., Granier, C., Peuch, V.-H., Rouil, L., Schultz, M.G., 2008. Toward a Monitoring and Forecasting System For Atmospheric Composition: The GEMS Project. Bull. Am. Meteorol. Soc. 89, 1147–1164. https://doi.org/10.1175/2008BAMS2355.1

Huneeus, N., Schulz, M., Balkanski, Y., Griesfeller, J., Prospero, M.J., Kinne, S., Bauer, S., Boucher, O., Chin, M., Dentener, F., 2011. Global dust model intercomparison in AeroCom phase I. Atmos. Chem. Phys. 11, 7781–7816.

Inness, A., Baier, F., Benedetti, A., Bouarar, I., Chabrillat, S., Clark, H., Clerbaux, C., Coheur, P., Engelen, R.J., Errera, Q., 2013a. The MACC reanalysis: an 8 yr data set of atmospheric composition. Atmos. Chem. Phys. 13, 4073–4109.

[dataset] Inness, A., Baier, F., Benedetti, A., Bouarar, I., Chabrillat, S., Clark, H., Clerbaux, C., Coheur, P., Engelen, R.J., Errera, Q., 2013b. The MACC reanalysis: an 8 yr data set of atmospheric composition. Atmos. Chem. Phys. 13, 4073–4109. (accessed 6 Feb 2018) http://apps.ecmwf.int/datasets/data/macc-reanalysis/levtype=sfc/

Kim, K.W., Kim, Y.J., Oh, S.J., 2001. Visibility impairment during Yellow Sand periods in the urban atmosphere of Kwangju, Korea. Atmos. Environ. 35, 5157–5167.

Kinne, S., Schulz, M., Textor, C., Guibert, S., Balkanski, Y., Bauer, S.E., Berntsen, T., Berglen, T.F., Boucher, O., Chin, M., 2005. An AeroCom initial assessment–optical

ACCEPTED MANUSCRIPT

properties in aerosol component modules of global models. Atmos. Chem. Phys. Discuss. 5, 8285–8330.

Levy, R.C., Remer, L.A., Kleidman, R.G., Mattoo, S., Ichoku, C., Kahn, R., Eck, T.F., 2010. Global evaluation of the Collection 5 MODIS dark-target aerosol products over land. Atmos. Chem. Phys. 10, 10399–10420.

Leys, J.F., Heidenreich, S.K., Strong, C.L., McTainsh, G.H., Quigley, S., 2011. PM10 concentrations and mass transport during "Red Dawn" – Sydney 23 September 2009. Aeolian Res. https://doi.org/https://doi.org/10.1016/j.aeolia.2011.06.003

Leys, J., McTainsh, G., Strong, C., Heidenreich, S., Biesaga, K., 2008. DustWatch: using community networks to improve wind erosion monitoring in Australia. Earth Surf. Process. Landforms 33, 1912–1926. https://doi.org/10.1002/esp.1733

Marx, S.K., McGowan, H.A., Kamber, B.S., 2009. Long-range dust transport from eastern Australia: A proxy for Holocene aridity and ENSO-type climate variability. Earth Planet. Sci. Lett. https://doi.org/https://doi.org/10.1016/j.epsl.2009.03.013

McTainsh, G.H., Lynch, A.W., Tews, E.K., 1998. Climatic controls upon dust storm occurrence in eastern Australia. J. Arid Environ. https://doi.org/https://doi.org/10.1006/jare.1997.0373

Mitchell, R.M., Campbell, S.K., Qin, Y., Gras, J.L., 2009. Performance Characteristics of Integrating Nephelometers in the Australian Outback. J. Atmos. Ocean. Technol. 26, 984–995. https://doi.org/10.1175/2008JTECHA1187.1

Mitchell, R.M., Campbell, S.K., Qin, Y., 2010. Recent increase in aerosol loading over the Australian arid zone. Atmos. Chem. Phys. 10, 1689–1699.

Mitchell, R.M., Forgan, B.W., Campbell, S.K., 2017. The Climatology of Australian Aerosol. Atmos. Chem. Phys. 17, 5131–5154.

Molod, A., Takacs, L., Suarez, M., Bacmeister, J., 2015. Development of the GEOS-5 atmospheric general circulation model: Evolution from MERRA to MERRA2. Geosci. Model Dev. 8, 1339.

Morcrette, J.-J., Beljaars, A., Benedetti, A., Jones, L., Boucher, O., 2008. Sea-salt and dust aerosols in the ECMWF IFS model. Geophys. Res. Lett. 35, n/a-n/a. https://doi.org/10.1029/2008GL036041

Morcrette, J.-J., Boucher, O., Jones, L., Salmond, D., Bechtold, P., Beljaars, A., Benedetti, A., Bonet, A., Kaiser, J.W., Razinger, M., Schulz, M., Serrar, S., Simmons, A.J., Sofiev, M., Suttie, M., Tompkins, A.M., Untch, A., 2009. Aerosol analysis and forecast in the European Centre for Medium-Range Weather Forecasts Integrated Forecast System: Forward modeling. J. Geophys. Res. Atmos. 114, n/a-n/a. https://doi.org/10.1029/2008JD011235

Mukkavilli, S.K., Prasad, A.A., Taylor, R.A., Troccoli, A., Kay, M.J., 2017. Mesoscale simulations of Australian direct normal irradiance, featuring an extreme dust event. J. Appl. Meteorol. Climatol. https://doi.org/10.1175/JAMC-D-17-0091.1

O'Loingsigh, T., Mitchell, R.M., Campbell, S.K., Drake, N.A., McTainsh, G.H., Tapper, N.J., Dunkerley, D.L., 2015a. Correction of dust event frequency from MODIS Quick-Look imagery using in-situ aerosol measurements over the Lake Eyre Basin, Australia. Remote Sens. Environ. https://doi.org/https://doi.org/10.1016/j.rse.2015.08.010

O'Loingsigh, T., McTainsh, G.H., Parsons, K., Strong, C.L., Shinkfield, P., Tapper, N.J., 2015b. Using meteorological observer data to compare wind erosion during two great droughts in eastern Australia; the World War II Drought (1937–1946) and the Millennium Drought (2001–2010). Earth Surf. Process. Landforms 40, 123–130. https://doi.org/10.1002/esp.3668

Perry, M., Troccoli, A., 2015. Impact of a fire burn on solar irradiance and PV power. Sol. Energy. https://doi.org/https://doi.org/10.1016/j.solener.2015.01.005

Qin, Y., Mitchell, R., Forgan, B.W., 2015. Characterizing the Aerosol and Surface Reflectance Over Australia Using AATSR. IEEE Trans. Geosci. Remote Sens. 53, 6163–6182. https://doi.org/10.1109/TGRS.2015.2433911

Randles, C.A., da Silva, A.M., Buchard, V., Colarco, P.R., Darmenov, A., Govindaraju, R., Smirnov, A., Holben, B., Ferrare, R., Hair, J., Shinozuka, Y., Flynn, C.J., 2017. The MERRA-2 Aerosol Reanalysis, 1980 Onward. Part I: System Description and Data Assimilation Evaluation. J. Clim. 30, 6823–6850. https://doi.org/10.1175/JCLI-D-16-0609.1

Remer, L.A., Kaufman, Y.J., Tanré, D., Mattoo, S., Chu, D.A., Martins, J. V, Li, R.-R., Ichoku, C., Levy, R.C., Kleidman, R.G., Eck, T.F., Vermote, E., Holben, B.N., 2005. The MODIS Aerosol Algorithm, Products, and Validation. J. Atmos. Sci. 62, 947–973. https://doi.org/10.1175/JAS3385.1

Remer, L.A., Kleidman, R.G., Levy, R.C., Kaufman, Y.J., Tanré, D., Mattoo, S., Martins, J.V., Ichoku, C., Koren, I., Yu, H., Holben, B.N., 2008. Global aerosol climatology from the MODIS satellite sensors. J. Geophys. Res. Atmos. 113, n/a-n/a. https://doi.org/10.1029/2007JD009661

Revel-Rolland, M., De Deckker, P., Delmonte, B., Hesse, P.P., Magee, J.W., Basile-Doelsch, I., Grousset, F., Bosch, D., 2006. Eastern Australia: A possible source of dust in East Antarctica interglacial ice. Earth Planet. Sci. Lett. https://doi.org/https://doi.org/10.1016/j.epsl.2006.06.028

Ridley, D.A., Heald, C.L., Kok, J.F., Zhao, C., 2016. An observationally constrained estimate of global dust aerosol optical depth. Atmos. Chem. Phys. 16, 15097–15117. https://doi.org/10.5194/acp-16-15097-2016

[dataset] Ridley, D.A., Heald, C.L., Kok, J.F., Zhao, C., 2016. An observationally constrained estimate of global dust aerosol optical depth. Atmos. Chem. Phys. 16, 15097–15117. https://doi.org/10.5194/acp-16-15097-2016

Rotstayn, L.D., Collier, M.A., Mitchell, R.M., Qin, Y., Campbell, S.K., Dravitzki, S.M., 2011. Simulated enhancement of ENSO-related rainfall variability due to Australian dust. Atmos. Chem. Phys. 11, 6575–6592.

Rotstayn, L.D., Jeffrey, S.J., Collier, M.A., Dravitzki, S.M., Hirst, A.C., Syktus, J.I., Wong, K.K., 2012. Aerosol-and greenhouse gas-induced changes in summer rainfall and

ACCEPTED MANUSCRIPT

ACCEPTED MANUSCRIPT

circulation in the Australasian region: a study using single-forcing climate simulations. Atmos. Chem. Phys. 12, 6377.

Shao, Y., Wyrwoll, K.-H., Chappell, A., Huang, J., Lin, Z., McTainsh, G.H., Mikami, M., Tanaka, T.Y., Wang, X., Yoon, S., 2011. Dust cycle: An emerging core theme in Earth system science. Aeolian Res. https://doi.org/https://doi.org/10.1016/j.aeolia.2011.02.001

Strong, C.L., Parsons, K., McTainsh, G.H., Sheehan, A., 2011. Dust transporting wind systems in the lower Lake Eyre Basin, Australia: A preliminary study. Aeolian Res. https://doi.org/https://doi.org/10.1016/j.aeolia.2010.11.001

Szczepanik, D., Markowicz, K.M., 2018. The relation between columnar and surface aerosol optical properties in a background environment. Atmos. Pollut. Res. https://doi.org/https://doi.org/10.1016/j.apr.2017.10.001

Tanaka, T.Y., Chiba, M., 2006. A numerical study of the contributions of dust source regions to the global dust budget. Monit. Model. Asian Dust Storms. https://doi.org/https://doi.org/10.1016/j.gloplacha.2006.02.002

Toll, V., Gleeson, E., Nielsen, K.P., Männik, A., Mašek, J., Rontu, L., Post, P., 2016. Impacts of the direct radiative effect of aerosols in numerical weather prediction over Europe using the ALADIN-HIRLAM NWP system. Atmos. Res. https://doi.org/https://doi.org/10.1016/j.atmosres.2016.01.003

Textor, C., Schulz, M., Guibert, S., Kinne, S., Balkanski, Y., Bauer, S., Berntsen, T., Berglen, T., Boucher, O., Chin, M., 2006. Analysis and quantification of the diversities of aerosol life cycles within AeroCom. Atmos. Chem. Phys. 6, 1777–1813.

Zhu, C.-S., Cao, J.-J., Ho, K.-F., Antony Chen, L.-W., Huang, R.-J., Wang, Y.-C., Li, H., Shen, Z.-X., Chow, J.C., Watson, J.G., Su, X., Wang, Q., Xiao, S., 2015. The optical properties of urban aerosol in northern China: A case study at Xi'an. Atmos. Res. https://doi.org/https://doi.org/10.1016/j.atmosres.2015.03.008

ACCEPTED MANUSCRIPT

ACCEPTED MANUSCRIPT

Abstract

Assessments of atmospheric aerosols from reanalysis are important for understanding uncertainty in model simulations, and ultimately predictions, such as for solar power or air quality forecasts and assessments. This study intercompares total aerosol optical depth (AOD) and dust AOD (DAOD) from two global reanalyses datasets, the European Centre for Medium-Range Weather Forecasts (ECMWF) Monitoring Atmospheric Composition and Climate (MACC) and the NASA Modern-Era Retrospective Analysis for Research-2 (MERRA-2). These are evaluated against AeroSpan (Aerosol characterisation via Sun photometry: Australian Network) ground observations which forms part of the Aerosol Robotic Network (AERONET) over the Australian continent for the 2002-2012 period. During dust storms, AeroSpan/AERONET AOD measurements were missing due to cloud screening. To overcome validation limitations in sun photometry for dust events, a nephelometer's scattering coefficient is qualitatively compared against reanalysis of DAOD at a key dust storm activation site, Tinga Tingana in South Australia (~200km east of Lake Eyre). A specific extreme event that occurred in 2009 originating from the Lake Eyre basin, a major dust source covering one-sixth of Australia, was studied. The results show that MERRA-2 reanalysis overestimates monthly total AOD twice as much compared to AeroSpan/AERONET ground observations but seems better correlated against AeroSpan/AERONET than ECMWF/MACC. Mean data of MERRA-2 time series over 10 years provide lower DAOD values and lower dust aerosol estimates than ECMWF/MACC reanalysis (over the Lake Eyre basin with spatial averaging). Specifically at Tinga Tingana, the correlation from MERRA-2 (0.45 correlation) and ECMWF/MACC (0.43 correlation) against AeroSpan/AERONET's AOD were similar. Between MERRA-2 and ECMWF/MACC decade long daily gridded DAOD, the correlation coefficient was high at 0.73, again indicating similarity between the datasets. MERRA-2 total AOD correlation is significantly higher (by 0.26) against AeroSpan/AERONET than ECMWF/MACC. MERRA-2 also provides higher AOD values in extreme cases which may correspond to dust storms.

ACCEPTED MANUSCRIPT

During dust storms, a hybrid strategy using nephelometers and hourly reanalysis from MERRA-2 is able to identify dust storms better than AeroSpan/AERONET. Overall, this work can enable and inform better aerosol data assimilation into forecast models such as for solar energy, agriculture or air quality over Australia.

ACCEPTED MANUSCRIPT

ACCEPTED MANUSCRIPT

Highlights

- Total and dust MERRA-2 and MACC reanalyses AOD analysed against Australian AERONET
- Dust AOD highest in summer; concentrated over Lake Eyre basin; seasonal differences
- Moderate 10-yr reanalyses dust AOD correlation ~0.44; monthly AOD two times AERONET
- MERRA-2 and MACC show significant total AOD differences by up to 0.26 with AERONET
- To detect dust storms recommend MERRA-2 hourly; nephelometer plus AERONET level 1.5

ACCEPTED MANUSCRIPT